

# Dissipativity-Based Synthesis of Distributed Control and Communication Topology Co-Design for AC Microgrids

Mohammad Javad Najafirad, Shirantha Welikala, Lei Wu, and Panos J. Antsaklis

**Abstract**—This paper presents a novel dissipativity-based framework for co-designing distributed controllers and communication topologies in AC microgrids (MGs). Unlike existing methods that treat control synthesis and topology design separately, we propose a unified approach that simultaneously optimizes both aspects to achieve voltage and frequency regulation and proportional power sharing among distributed generators (DGs). We formulate the closed-loop AC MG as a networked system where DGs, distribution lines, and loads are interconnected subsystems characterized by their dissipative properties. Each DG employs a hierarchical architecture combining local controllers for voltage regulation and distributed controllers for droop-free power sharing through normalized power consensus. By leveraging dissipativity theory, we establish necessary and sufficient conditions for subsystem passivity and cast the co-design problem as a convex linear matrix inequality (LMI) optimization, enabling efficient computation and guaranteed stability. Our framework systematically synthesizes sparse communication topologies while handling the coupled dq-frame dynamics and dual power flow objectives inherent to AC MGs. Simulation results on a representative AC MG demonstrate the effectiveness of the proposed approach in achieving accurate voltage regulation, frequency synchronization, and proportional power sharing.

**Index Terms**—AC Microgrid, Voltage Regulation, Distributed Control, Networked Systems, Dissipativity-Based Control, Topology Design.

## I. INTRODUCTION

The integration of renewable energy sources into power systems has accelerated the development of microgrids (MGs) as a reliable solution for electric energy sustainability. AC MGs, in particular, have emerged as critical components of modern power infrastructure and provide enhanced flexibility to manage distributed generators (DGs), energy storage systems, and various load types within localized networks [1]. Nevertheless, the control architecture of AC MGs faces significant challenges to maintain voltage stability, frequency synchronization, and proportional power sharing among DGs, particularly in islanded operation where no utility grid support is available [2]. These challenges become more complex due to the inherent nature of AC systems, which must manage both active and reactive power flows while multiple DGs operate in parallel synchronization [3]. Recent advances in networked control theory and communication technologies have opened new avenues to

Mohammad Javad Najafirad, Shirantha Welikala, and Lei Wu are with the Department of Electrical and Computer Engineering, School of Engineering and Science, Stevens Institute of Technology, Hoboken, NJ 07030,  [{mnajafir, swelikal, lei.wu}@stevens.edu](mailto:{mnajafir, swelikal, lei.wu}@stevens.edu). Panos J. Antsaklis is with the Department of Electrical Engineering, University of Notre Dame, Notre Dame, IN 46556,  [pantsakl@nd.edu](mailto:pantsakl@nd.edu).

develop sophisticated control strategies that address these multifaceted challenges through coordinated operation rather than purely local control actions [4].

Traditional control strategies for AC MGs have evolved from centralized to decentralized and distributed approaches to address scalability and reliability concerns [5]. Centralized control offers precise coordination but suffers from single points of failure and communication bottlenecks, while fully decentralized methods sacrifice optimal performance for local autonomy [6]. Distributed control emerges as a balanced solution that enables DGs to coordinate through sparse communication networks while each unit maintains local control authority [7]. The challenge lies in the design of both the control algorithms and the communication topology to achieve desired performance objectives. Most existing distributed control methods assume predetermined communication structures that mirror the physical electrical connections, which may not offer optimal information exchange patterns [8]. Furthermore, the complex nature of AC systems requires careful consideration of both voltage magnitude and phase angle dynamics, as well as the coupled relationship between active and reactive power flows [9].

Dissipativity theory provides a powerful framework to analyze and design control systems for interconnected networks by characterizing subsystems through their energy exchange properties [10]. Unlike traditional Lyapunov methods that require detailed system models, dissipativity-based approaches need only input-output energy relationships, greatly simplifying the analysis of complex networked systems [11]. Recent applications to AC MGs have shown promise in addressing voltage stabilization and power quality issues through passivity-based methods, though most approaches still rely on predetermined control structures without considering communication optimization [12]. The compositional nature of dissipativity theory allows modular design where individual DG controllers can be synthesized independently while guaranteeing overall system stability, a critical feature for scalable AC MG architectures [9]. However, the extension to comprehensive AC system control presents unique challenges due to the coupling between voltage components in the *dq* reference frame, the inherent complexity of three-phase power systems, and the need to manage both active and reactive power flows [13]. The ability to guarantee stability through compositional certification makes dissipativity particularly attractive for modular AC MG architectures.

Despite these theoretical advances, most existing distributed control methods for AC MGs treat controller design and communication topology as separate problems,

potentially missing optimal solutions that arise from their joint consideration [14]. Current approaches typically assume fixed communication structures or require all-to-all information exchange, which becomes impractical as MG size increases [15]. Moreover, simultaneously achieving voltage regulation and proportional power sharing in AC systems requires careful coordination of both active and reactive power controllers, a challenge not fully addressed by existing methods [16]. The need for a systematic co-design framework that jointly optimizes control parameters and communication topology while guaranteeing stability through rigorous theoretical foundations motivates this work.

This paper presents a novel dissipativity-based control and communication topology co-design framework for AC MGs with the following contributions:

- 1) We formulate the AC MG control problem as a networked system where DGs and distribution lines are modeled as interconnected subsystems with specific dissipative properties.
- 2) We develop a unified LMI-based co-design methodology that simultaneously optimizes distributed controllers and communication topology for both active and reactive power sharing.
- 3) We establish necessary and sufficient conditions for subsystem passivity that ensure the feasibility of the global co-design problem.

This work builds upon the dissipativity-based framework established in [17] for DC MGs and the systematic co-design methodology developed in [18] for vehicular platoons, extending these concepts to address the unique challenges of AC MG control with coupled  $dq$  dynamics and dual power flow objectives.

## II. PRELIMINARIES

**Notations:** Notations  $\mathbb{R}$  and  $\mathbb{N}$  respectively signify the sets of real and natural numbers. For any  $N \in \mathbb{N}$ , we define  $\mathbb{N}_N \triangleq \{1, 2, \dots, N\}$ . An  $n \times m$  block matrix  $A$  is denoted as  $A = [A_{ij}]_{i \in \mathbb{N}_N, j \in \mathbb{N}_m}$ . Either subscripts or superscripts are used for indexing purposes, e.g.,  $A_{ij} = A^{ij}$ .  $[A_{ij}]_{j \in \mathbb{N}_m}$  and  $\text{diag}([A_{ii}]_{i \in \mathbb{N}_N})$  respectively represent a block row matrix and a block diagonal matrix.  $\mathbf{0}$  and  $\mathbf{I}$  are the zero and identity matrices, with proper dimensions clear from the context. A symmetric positive definite (semi-definite) matrix  $A \in \mathbb{R}^{n \times n}$  is denoted by  $A > 0$  ( $A \geq 0$ ). The symbol  $\star$  represents conjugate blocks inside block symmetric matrices.  $\mathcal{H}(A) \triangleq A + A^\top$ .  $\mathbf{1}_{\{\cdot\}}$  is the indicator function.

### A. Dissipativity

Consider a general non-linear dynamic system

$$\begin{aligned} \dot{x}(t) &= f(x(t), u(t)), \\ y(t) &= h(x(t), u(t)), \end{aligned} \quad (1)$$

where  $x(t) \in \mathbb{R}^n$ ,  $u(t) \in \mathbb{R}^q$ ,  $y(t) \in \mathbb{R}^m$ , and  $f : \mathbb{R}^n \times \mathbb{R}^q \rightarrow \mathbb{R}^n$  and  $h : \mathbb{R}^n \times \mathbb{R}^q \rightarrow \mathbb{R}^m$  are continuously differentiable. The equilibrium points of (1) are such that there is a unique  $u^* \in \mathbb{R}^q$  that meets  $f(x^*, u^*) = 0$  for any  $x^* \in \mathcal{X}$ , where

$\mathcal{X} \subset \mathbb{R}^n$  is the set of equilibrium states. Both  $u^*$  and  $y^* \triangleq h(x^*, u^*)$  are implicit functions of  $x^*$ .

The *equilibrium-independent-dissipativity* (EID) [19] is defined next to examine dissipativity of (1) without the explicit knowledge of its equilibrium points.

**Definition 1:** The system (1) is called EID under supply rate  $s : \mathbb{R}^q \times \mathbb{R}^m \rightarrow \mathbb{R}$  if there is a continuously differentiable storage function  $V : \mathbb{R}^n \times \mathcal{X} \rightarrow \mathbb{R}$  such that  $V(x, x^*) > 0$  when  $x \neq x^*$ ,  $V(x^*, x^*) = 0$ , and  $\dot{V}(x, x^*) = \nabla_x V(x, x^*) f(x, u) \leq s(u - u^*, y - y^*)$ , for all  $(x, x^*, u) \in \mathbb{R}^n \times \mathcal{X} \times \mathbb{R}^q$ .

This EID property can be specialized based on the used supply rate  $s(\cdot, \cdot)$ . The  $X$ -EID property, defined in the sequel, uses a quadratic supply rate determined by a coefficient matrix  $X = X^\top \triangleq [X^{kl}]_{k, l \in \mathbb{N}_2} \in \mathbb{R}^{q+m}$  [20].

**Definition 2:** The system (1) is  $X$ -EID if it is EID under the quadratic supply rate:

$$s(u - u^*, y - y^*) \triangleq \begin{bmatrix} u - u^* \\ y - y^* \end{bmatrix}^\top \begin{bmatrix} X^{11} & X^{12} \\ X^{21} & X^{22} \end{bmatrix} \begin{bmatrix} u - u^* \\ y - y^* \end{bmatrix}.$$

**Remark 1:** If the system (1) is  $X$ -EID with:

- 1)  $X = \begin{bmatrix} \mathbf{0} & \frac{1}{2}\mathbf{I} \\ \frac{1}{2}\mathbf{I} & \mathbf{0} \end{bmatrix}$ , then it is passive;
- 2)  $X = \begin{bmatrix} -\nu\mathbf{I} & \frac{1}{2}\mathbf{I} \\ \frac{1}{2}\mathbf{I} & -\rho\mathbf{I} \end{bmatrix}$ , then it is strictly passive ( $\nu$  and  $\rho$  are the input and output passivity indices, denoted as IF-OFP( $\nu, \rho$ ));
- 3)  $X = \begin{bmatrix} \gamma^2\mathbf{I} & \mathbf{0} \\ \mathbf{0} & -\mathbf{I} \end{bmatrix}$ , then it is  $L_2$ -stable ( $\gamma$  is the  $L_2$ -gain, denoted as  $L2G(\gamma)$ );

in an equilibrium-independent manner (see also [21]).

If the system (1) is linear time-invariant (LTI), a necessary and sufficient condition for  $X$ -EID is provided in the following proposition as an LMI problem.

**Proposition 1:** [18] The LTI system

$$\dot{x}(t) = Ax(t) + Bu(t), \quad y(t) = Cx(t) + Du(t),$$

is  $X$ -EID if and only if there exists  $P > 0$  such that

$$\begin{bmatrix} -\mathcal{H}(PA) + C^\top X^{22}C & -PB + C^\top X^{21} + C^\top X^{22}D \\ * & X^{11} + \mathcal{H}(X^{12}D) + D^\top X^{22}D \end{bmatrix} \geq 0.$$

### B. Networked Systems

Consider the networked system  $\Sigma$  that consists of dynamic subsystems  $\Sigma_i, i \in \mathbb{N}_N$  and  $\bar{\Sigma}_i, i \in \mathbb{N}_{\bar{N}}$  which are linked via a static interconnection matrix  $M$ , with the exogenous inputs  $w(t) \in \mathbb{R}^r$  (e.g. disturbances) and interested outputs  $z(t) \in \mathbb{R}^l$  (e.g. performance).

The dynamics of each subsystem  $\Sigma_i, i \in \mathbb{N}_N$  are given by

$$\begin{aligned} \dot{x}_i(t) &= f_i(x_i(t), u_i(t)), \\ y_i(t) &= h_i(x_i(t), u_i(t)), \end{aligned} \quad (2)$$

where  $x_i(t) \in \mathbb{R}^{n_i}$ ,  $u_i(t) \in \mathbb{R}^{q_i}$ ,  $y_i(t) \in \mathbb{R}^{m_i}$ . Similar to (1), each subsystem  $\Sigma_i, i \in \mathbb{N}_N$  is considered to have a set  $\mathcal{X}_i \subset \mathbb{R}^{n_i}$ , where for every  $x_i^* \in \mathcal{X}_i$ , there exists a unique  $u_i^* \in \mathbb{R}^{q_i}$  such that  $f_i(x_i^*, u_i^*) = 0$ , and both  $u_i^*$  and  $y_i^* \triangleq h_i(x_i^*, u_i^*)$  are implicit function of  $x_i^*$ . Moreover, each subsystem  $\Sigma_i, i \in \mathbb{N}_N$  is assumed to be  $X_i$ -EID, where  $X_i \triangleq [X_i^{kl}]_{k, l \in \mathbb{N}_2}$ . Regarding each subsystem  $\bar{\Sigma}_i, i \in \mathbb{N}_{\bar{N}}$ , we use similar assumptions and notations, but include a bar symbol to highlight that  $\bar{\Sigma}_i$  is  $\bar{X}_i$ -EID where  $\bar{X}_i \triangleq [\bar{X}_i^{kl}]_{k, l \in \mathbb{N}_2}$ .

Defining  $u \triangleq [u_i^\top]_{i \in \mathbb{N}_N}^\top$ ,  $y \triangleq [y_i^\top]_{i \in \mathbb{N}_N}^\top$ ,  $\bar{u} \triangleq [\bar{u}_i^\top]_{i \in \mathbb{N}_{\bar{N}}}^\top$  and  $\bar{y} \triangleq [y_i^\top]_{i \in \mathbb{N}_{\bar{N}}}^\top$ , the interconnection matrix  $M$  and the

corresponding interconnection relationship are given by

$$\begin{bmatrix} u \\ \bar{u} \\ z \end{bmatrix} = M \begin{bmatrix} y \\ \bar{y} \\ w \end{bmatrix} \equiv \begin{bmatrix} M_{uy} & M_{u\bar{y}} & M_{uw} \\ M_{\bar{u}y} & M_{\bar{u}\bar{y}} & M_{\bar{u}w} \\ M_{zy} & M_{z\bar{y}} & M_{zw} \end{bmatrix} \begin{bmatrix} y \\ \bar{y} \\ w \end{bmatrix}. \quad (3)$$

The following proposition exploits the  $X_i$ -EID and  $\bar{X}_i$ -EID properties of the subsystems  $\Sigma_i, i \in \mathbb{N}_N$  and  $\bar{\Sigma}_i, i \in \mathbb{N}_{\bar{N}}$  to formulate an LMI problem for synthesizing the interconnection matrix  $M$  (3), ensuring the networked system  $\Sigma$  is  $\mathbf{Y}$ -EID for a prespecified  $\mathbf{Y}$  under two mild assumptions [20].

**Assumption 1:** For the networked system  $\Sigma$ , the provided  $\mathbf{Y}$ -EID specification is such that  $\mathbf{Y}^{22} < 0$ .

**Remark 2:** Based on Rm. 1, Assumption 1 holds if the networked system  $\Sigma$  must be either: (i) L2G( $\gamma$ ) or (ii) IF-OFP( $\nu, \rho$ ) with some  $\rho > 0$ , i.e.,  $L_2$ -stable or passive, respectively. Therefore, Assumption 1 is mild since it is usually preferable to make the networked system  $\Sigma$  either  $L_2$ -stable or passive.

**Assumption 2:** In the networked system  $\Sigma$ , each subsystem  $\Sigma_i$  is  $X_i$ -EID with  $X_i^{11} > 0, \forall i \in \mathbb{N}_N$ , and similarly, each subsystem  $\bar{\Sigma}_i$  is  $\bar{X}_i$ -EID with  $\bar{X}_i^{11} > 0, \forall i \in \mathbb{N}_{\bar{N}}$ .

**Remark 3:** According to Rm. 1, Assumption 2 holds if a subsystem  $\Sigma_i, i \in \mathbb{N}_N$  is either: (i) L2G( $\gamma_i$ ) or (ii) IF-OFP( $\nu_i, \rho_i$ ) with  $\nu_i < 0$  (i.e.,  $L_2$ -stable or non-passive). Since in passivity-based control, often the involved subsystems are non-passive (or can be treated as such), Assumption 2 is also mild.

**Proposition 2:** [20] Under Assumptions 1 and 2, the network system  $\Sigma$  can be made  $\mathbf{Y}$ -EID (from  $w(t)$  to  $z(t)$ ) by synthesizing the interconnection matrix  $M$  through solving the LMI problem:

Find:  $L_{uy}, L_{u\bar{y}}, L_{uw}, L_{\bar{u}y}, L_{\bar{u}w}, M_{zy}, M_{z\bar{y}}$ , and  $M_{zw}$ ,  
s.t.:  $p_i \geq 0, \forall i \in \mathbb{N}_N$ ,  $\bar{p}_l \geq 0, \forall l \in \mathbb{N}_{\bar{N}}$ , and (5),  
(4)

with  $\begin{bmatrix} M_{uy} & M_{u\bar{y}} & M_{uw} \\ M_{\bar{u}y} & M_{\bar{u}\bar{y}} & M_{\bar{u}w} \end{bmatrix} = \begin{bmatrix} \mathbf{X}_p^{11} & \mathbf{0} \\ \mathbf{0} & \bar{\mathbf{X}}_{\bar{p}}^{11} \end{bmatrix}^{-1} \begin{bmatrix} L_{uy} & L_{u\bar{y}} & L_{uw} \\ L_{\bar{u}y} & L_{\bar{u}\bar{y}} & L_{\bar{u}w} \end{bmatrix}$ , where  $\mathbf{X}_p^{11} = \text{diag}(\{p_i X_i^{11} : i \in \mathbb{N}_N\})$ ,  $\bar{\mathbf{X}}_{\bar{p}}^{11} = \text{diag}(\{\bar{p}_i \bar{X}_i^{11} : i \in \mathbb{N}_{\bar{N}}\})$ ,  $\mathbf{X}^{12} \triangleq \text{diag}((X_i^{11})^{-1} X_i^{12} : i \in \mathbb{N}_N)$ ,  $\mathbf{X}^{21} \triangleq (\mathbf{X}^{12})^\top$ ,  $\bar{\mathbf{X}}^{12} \triangleq \text{diag}((\bar{X}_i^{11})^{-1} \bar{X}_i^{12} : i \in \mathbb{N}_{\bar{N}})$ , and  $\bar{\mathbf{X}}^{21} \triangleq (\bar{\mathbf{X}}^{12})^\top$ .

### III. SYSTEM MODELING

This section presents the dynamic modeling of the AC MG, which consists of multiple DGs, loads, and power distribution lines. Our modeling approach is motivated by [22], which demonstrates the effectiveness of passivity-based analysis for voltage and frequency stabilization in islanded AC MGs. Building upon their electrical modeling framework, we extend the analysis to include power flow relationships and distributed coordination mechanisms. We introduce both local voltage controllers and distributed power sharing controllers for the AC MG and represent the closed-

loop AC MG as a networked system suitable for dissipativity-based analysis.

#### A. AC MG Topology

The physical interconnection topology of an AC MG is modeled as a directed connected graph  $\mathcal{G}^p = (\mathcal{V}, \mathcal{E})$ .  $\mathcal{V}$  is partitioned into two sets:  $\mathcal{M} = \{1, \dots, N+M\}$  represents DGs  $\mathcal{D} = \{1, \dots, N\}$  and loads  $\mathcal{L} = \{N+1, \dots, N+M\}$  with  $\mathcal{M} = \mathcal{D} \cup \mathcal{L}$ , and  $\mathcal{P} = \{N+M+1, \dots, N+M+L\}$  is the set of distribution lines. Individual DGs and loads are interfaced with the AC MG through a point of common coupling (PCC), see Fig. 1 for a representative AC MG diagram. The orientation of each edge represents the reference direction of positive currents, which is arbitrarily assigned. A line cannot have only in-neighbors or out-neighbors, as the current entering in a line must leave it. Indeed, each node in  $\mathcal{P}$  is always connected to two distinct nodes in  $\mathcal{M}$  through two directed edges. We define a matrix  $\mathcal{B} \in \mathbb{R}^{(N+M) \times L}$ , with DGs and loads along rows and lines along columns, as

$$\mathcal{B}_{kl} = \begin{cases} 1 & l \in \mathcal{E}_k^+ \\ -1 & l \in \mathcal{E}_k^- \\ 0 & \text{otherwise} \end{cases}, \quad k \in \mathcal{M}, l \in \mathcal{P}, \quad (6)$$

where  $\mathcal{E}_k^+ = \{l \in \mathcal{V} : (k, l) \in \mathcal{E}\}$  denotes the set of out-neighbors,  $\mathcal{E}_k^- = \{j \in \mathcal{V} : (j, k) \in \mathcal{E}\}$  the set of in-neighbors, and  $\mathcal{N}_k = \mathcal{E}_k^+ \cup \mathcal{E}_k^-$  the set of neighbors.

For analysis purposes in this paper, we define the following neighbor sets. For physical topology, each  $\Sigma_i^{DG}$  has a physical neighbor set  $\mathcal{N}_i^P = \{l : \mathcal{B}_{il} \neq 0\}$  representing the distribution lines connected to  $\Sigma_i^{DG}$ . Similarly, each  $\Sigma_m^{load}$  has a physical neighbor set  $\mathcal{N}_m^P = \{l : \mathcal{B}_{ml} \neq 0\}$  representing the distribution lines connected to  $\Sigma_m^{load}$ . Conversely, each distribution line  $\Sigma_i^{line}$  has a physical neighbor set  $\mathcal{N}_i^P = \{k : \mathcal{B}_{kl} \neq 0\}$  representing the DGs and loads connected to  $\Sigma_i^{line}$ .

#### B. Dynamic Model of a DG

Each DG comprises a DC voltage source, a voltage source converter (VSC), and series RLC filter components. The  $\{\Sigma_i^{DG} : i \in \mathbb{N}_N\}$  supplies power to local loads in its PCC $_i$  while maintaining interconnection with other DG units through distribution lines  $\{\Sigma_l^{line} : l \in \mathcal{E}_i\}$ . Figure 2 illustrates the electrical schematic of  $\Sigma_i^{DG}$ , including the DG, local loads, and connected distribution line.

Motivated by the modeling approach in [22], we represent all three-phase electrical signals in a common direct and quadrature axis ( $dq$ ) reference frame rotating at the nominal network frequency  $\omega_0$ . This representation enables systematic control design while maintaining the coupling between  $dq$  components. By applying Kirchhoff's current law (KCL)

$$\begin{bmatrix} \mathbf{X}_p^{11} & \mathbf{0} & \mathbf{0} & L_{uy} \\ \mathbf{0} & \bar{\mathbf{X}}_{\bar{p}}^{11} & \mathbf{0} & L_{\bar{u}y} \\ \mathbf{0} & \mathbf{0} & -\mathbf{Y}^{22} & -\mathbf{Y}^{22} M_{zy} \\ L_{uy}^\top & L_{\bar{u}y}^\top & -M_{zy}^\top \mathbf{Y}^{22} & -L_{uy}^\top \mathbf{X}^{12} - \mathbf{X}^{21} L_{uy} - \mathbf{X}_p^{22} \\ L_{\bar{u}y}^\top & L_{\bar{u}\bar{y}}^\top & -M_{z\bar{y}}^\top \mathbf{Y}^{22} & -L_{\bar{u}y}^\top \mathbf{X}^{12} - \bar{\mathbf{X}}^{21} L_{\bar{u}y} \\ L_{uw}^\top & L_{\bar{u}w}^\top & -M_{zw}^\top \mathbf{Y}^{22} & -L_{uw}^\top \mathbf{X}^{12} + \mathbf{Y}^{12} M_{zy} \end{bmatrix} \begin{bmatrix} L_{u\bar{y}} \\ L_{\bar{u}\bar{y}} \\ -\mathbf{Y}^{22} M_{z\bar{y}} \\ -\mathbf{X}^{21} L_{uy} - L_{\bar{u}y} \bar{\mathbf{X}}^{12} \\ -(L_{\bar{u}y}^\top \bar{\mathbf{X}}^{12} + \bar{\mathbf{X}}^{21} L_{\bar{u}y} + \bar{\mathbf{X}}_{\bar{p}}^{22}) \\ -L_{\bar{u}w}^\top \bar{\mathbf{X}}^{12} + \mathbf{Y}^{12} M_{z\bar{y}} \\ L_{uw} \\ L_{\bar{u}w} \\ \mathbf{Y}^{22} M_{zw} \\ -\mathbf{X}^{21} L_{uw} + M_{zw}^\top \mathbf{Y}^{21} \\ -\bar{\mathbf{X}}^{21} L_{\bar{u}w} + M_{z\bar{y}}^\top \mathbf{Y}^{21} \\ M_{zw}^\top \mathbf{Y}^{21} + \mathbf{Y}^{12} M_{zw} + \mathbf{Y}^{11} \end{bmatrix} > 0 \quad (5)$$

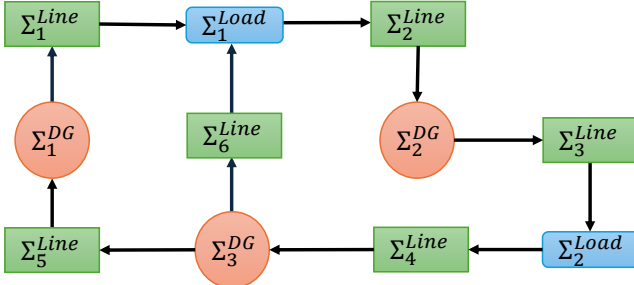


Fig. 1. A representative diagram of the AC MG network. The sets  $\mathcal{D}$ ,  $\mathcal{L}$ , and  $\mathcal{P}$  are represented as DGs, distribution lines and loads.

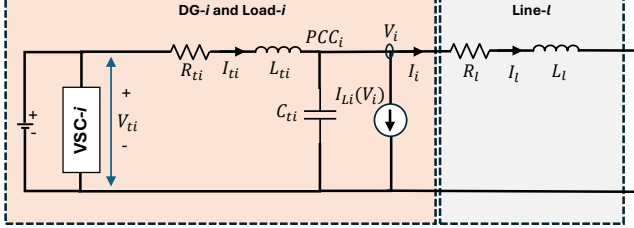


Fig. 2. Electrical scheme of DG  $i$  and distribution line  $l$  for AC MG.

at PCC $_i$  on the DG side, we obtain the following for  $\Sigma_i^{DG}$ :

$$\begin{aligned} C_{ti} \frac{dV_i^{dq}}{dt} &= -C_{ti}j\omega_0 V_i^{dq} + I_{ti}^{dq} - I_{Li}^{dq}(V_i^{dq}) - I_i^{dq}, \\ \frac{dI_{ti}^{dq}}{dt} &= -V_i^{dq} - (R_{ti} + L_{ti}j\omega_0) I_{ti}^{dq} + V_{ti}^{dq}, \end{aligned} \quad (7)$$

where  $V_i^{dq} = V_i^d + jV_i^q$ ,  $I_{ti}^{dq} = I_{ti}^d + jI_{ti}^q$ , and the net current injected into the AC MG by  $\Sigma_i^{DG}$  is given by:

$$I_i^{dq} = \sum_{l \in \mathcal{E}_i} \mathcal{B}_{il} I_l^{dq}. \quad (8)$$

The  $j\omega_0$  terms in (7) represent the cross-coupling between  $d$  and  $q$  components inherent in the rotating reference frame, where the  $+j\omega_0$  term coupling in the voltage equation corresponds to the natural dynamics of AC quantities in the synchronously rotating frame, while the  $-j\omega_0$  term in the current equation accounts for the inductance-based phase relationships.

In (7), the parameters  $R_{ti}$ ,  $L_{ti}$ , and  $C_{ti}$  represent the internal resistance, inductance, and filter capacitance of  $\Sigma_i^{DG}$ , respectively. The state variables are selected as  $V_i^d$ ,  $V_i^q$  (the  $dq$ -components of PCC $_i$  voltage) and  $I_{ti}^d$ ,  $I_{ti}^q$  (the  $dq$ -components of filter current). The term  $V_{ti}^{dq} = V_{ti}^d + jV_{ti}^q$  represents the control input command applied at the VSC,  $I_{Li}^{dq} = I_{Li}^d + jI_{Li}^q$  denotes the local load current, and  $I_i^{dq} = I_i^d + jI_i^q$  represents the total current injection to the AC MG by  $\Sigma_i^{DG}$ .

### C. Line Power Flow Calculation

The active and reactive power injections to the AC MG by each  $\Sigma_i^{DG}$  are denoted respectively as  $P_i$  and  $Q_i$ , which can be calculated via  $V_i^{dq}$  (PCC $_i$  voltage) and  $I_i^{dq}$  (total current injection (8)), as [23]:

$$\begin{aligned} P_i &= V_i^d I_i^d + V_i^q I_i^q, \\ Q_i &= V_i^q I_i^d - V_i^d I_i^q. \end{aligned} \quad (9)$$

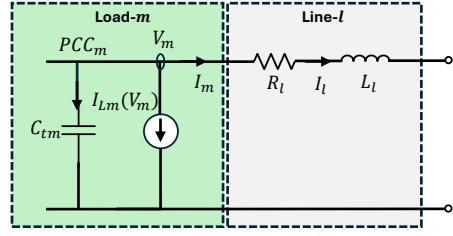


Fig. 3. Electrical scheme of ZIP load in AC MG.

This formulation provides direct calculation of power outputs without requiring explicit phase-angle tracking, thereby maintaining consistency with the single synchronously rotating reference frame. The calculated active and reactive power values serve as feedback signals for the distributed consensus-based control in Sec. IV-C, enabling proportional power sharing among DGs.

### D. Load Model

The loads in the AC MG are modeled as a combination of constant impedance ( $Z$ ), constant current ( $I$ ), and constant power ( $P$ ) components, commonly referred to as ZIP loads.

Each local load is connected at a DG terminal through its respective PCC. At  $\Sigma_i^{DG}$ , the local load current

$$I_{Li}^{dq} = I_{Li}^Z + I_{Li}^I + I_{Li}^P = Y_{Li} V_i^{dq} + \bar{I}_{Li}^{dq} + P_{Li}^{dq}, \quad (10)$$

where  $Y_{Li}$  represents the load admittance,  $\bar{I}_{Li}^{dq}$  denotes the constant current component, and  $P_{Li}^{dq}$  is the constant power component of the load.

On the other hand, the  $m$ -th global load  $\Sigma_m^{Load}$ , along with its connecting power lines (at PCC $_m$ ), is shown in Fig. 3. Similar to local loads, the total global load current comprises three components:

$$I_{Lm}^{dq} = I_{Lm}^Z + I_{Lm}^I + I_{Lm}^P = Y_{Lm} V_m^{dq} + \bar{I}_{Lm}^{dq} + P_{Lm}^{dq}, \quad (11)$$

where  $Y_{Lm}$  represents the load admittance,  $\bar{I}_{Lm}^{dq}$  denotes the constant current component, and  $P_{Lm}^{dq}$  is the constant power component of the load.

We consider the dynamic effects of global loads, particularly those arising from load filter capacitance. By applying KCL at PCC $_m$ , we obtain the dynamic model of the global load  $\Sigma_m^{Load}$  in  $dq$  frame as:

$$\frac{dV_m^{dq}}{dt} = -j\omega_0 V_m^{dq} - \frac{1}{C_{tm}} \left( Y_{Lm} V_m^{dq} + \bar{I}_{Lm}^{dq} + P_{Lm}^{dq} \right) - \frac{I_m^{dq}}{C_{tm}}, \quad (12)$$

where  $I_m^{dq}$  is the net current injection from connected distribution lines. The net current injected into the AC MG by  $\Sigma_m^{Load}$  is given by:

$$I_m^{dq} = \sum_{l \in \mathcal{E}_m} \mathcal{B}_{ml} I_l^{dq}. \quad (13)$$

The state space representation of  $\Sigma_m^{Load}$  is:

$$\dot{x}_m(t) = \check{A}_m \check{x}_m(t) + \check{B}_m \check{u}_m(t) + \check{B}_m \check{d}_m(t), \quad (14)$$

where the state vector is  $\check{x}_m = [V_m^d \ V_m^q]^\top$ , the exogenous input is  $\check{d}_m = [\bar{I}_{Lm}^d \ \bar{I}_{Lm}^q]^\top$  (which represents the constant current load component under the common assumption

$P_{Lm}^{dq} = 0$ ), and the coupling input is  $\bar{u}_m = [I_m^d \quad I_m^q]^\top$ . The system matrices  $\check{A}_m$  and  $\check{B}_m$  in (14) respectively are

$$\check{A}_m \triangleq \begin{bmatrix} -\frac{Y_{Lm}}{C_{tm}} & \omega_0 \\ -\omega_0 & -\frac{Y_{Lm}}{C_{tm}} \end{bmatrix}, \text{ and } \check{B}_m \triangleq \begin{bmatrix} -\frac{1}{C_{tm}} & 0 \\ 0 & -\frac{1}{C_{tm}} \end{bmatrix}. \quad (15)$$

### E. Distribution Line Model

Each distribution line is represented using  $\pi$ -equivalent circuit model, where the line capacitances are lumped with the DG filter capacitances at the connection points. Following the modeling approach in [22], the distribution line  $\Sigma_l^{line}$  is modeled as an RL circuit with resistance  $R_l$  and inductance  $L_l$ . By applying Kirchhoff's voltage law (KVL) to  $\Sigma_l^{line}$  we obtain its dynamic model in the  $dq$  reference frame as:

$$\frac{dI_l^{dq}}{dt} = -\left(\frac{R_l}{L_l} + j\omega_0\right)I_l^{dq} + \frac{1}{L_l} \sum_{i \in \mathcal{N}_l^P} \mathcal{B}_{il} V_i^{dq}, \quad (16)$$

where  $I_l^{dq} = I_l^d + jI_l^q$  represents the current flowing through  $\Sigma_l^{line}$ . The voltage difference across the line (which excites the line dynamics, also called the coupling input) is determined by the PCC voltages of the connected DGs/loads.

The distribution line dynamics capture the inductive and resistive effects in the  $dq$  frame while maintaining the coupling between  $d$  and  $q$  components through the  $\omega_0$  terms, which represent the natural dynamics of AC quantities in the synchronously rotating reference frame.

Separating the real and imaginary components, the state space representation of  $\Sigma_l^{line}$  can be obtained as:

$$\dot{\bar{x}}_l(t) = \bar{A}_l \bar{x}_l(t) + \bar{B}_l \bar{u}_l(t), \quad (17)$$

where the state vector is  $\bar{x}_l = [I_l^d \quad I_l^q]^\top$ , and the coupling input is

$$\bar{u}_l = \sum_{k \in \mathcal{N}_l^P} \mathcal{B}_{kl} [V_k^d \quad V_k^q]^\top. \quad (18)$$

The system matrices in (17) are:

$$\bar{A}_l \triangleq \begin{bmatrix} -\frac{R_l}{L_l} & \omega_0 \\ -\omega_0 & -\frac{R_l}{L_l} \end{bmatrix}, \quad \bar{B}_l \triangleq \begin{bmatrix} \frac{1}{L_l} & 0 \\ 0 & \frac{1}{L_l} \end{bmatrix}. \quad (19)$$

## IV. PROPOSED CONTROLLERS

The control architecture for the AC MG employs a hierarchical structure with three layers: local steady-state controllers for equilibrium point adjustment, local feedback controllers for voltage regulation at each  $\Sigma_i^{DG}$ , and distributed controllers for coordinated power sharing among DGs via communication networks. The local steady-state controllers ensure a proper operating equilibrium point for the AC MG, mitigating steady-state errors; the local feedback controllers ensure fast voltage tracking at each PCC; the distributed controllers ensure proportional power sharing by coordinating frequency references without centralized coordination.

### A. Local Feedback Controllers

Each DG is equipped with local feedback controllers that enable tracking a given PCC voltage reference. To achieve precise voltage tracking, each  $\Sigma_i^{DG}, i \in \mathbb{N}_N$  is augmented

with an integral voltage tracking error state  $v_i^{dq}$ , of which the dynamics are:

$$\dot{v}_i^{dq}(t) = e_i^{dq}(t) = V_i^{dq} - V_{i,ref}^{dq}, \quad (20)$$

where  $v_i^{dq} = v_i^d + jv_i^q$  represents the  $dq$  components of the integral voltage tracking error, and  $V_{i,ref}^{dq} = V_{i,ref}^d + jV_{i,ref}^q$  is a prespecified voltage reference.

Consequently, each  $\Sigma_i^{DG}$  is equipped with a PI-structured local feedback controller  $u_{iL}(t)$  that uses only voltage measurements and integral states:

$$\begin{aligned} u_{iL}(t) &\triangleq K_i^P \begin{bmatrix} e_i^d(t) \\ e_i^q(t) \end{bmatrix} + K_i^I \int_0^t \begin{bmatrix} e_i^d(\tau) \\ e_i^q(\tau) \end{bmatrix} d\tau \\ &= K_{i0} x_i(t) - K_i^P \begin{bmatrix} V_{i,ref}^d \\ V_{i,ref}^q \end{bmatrix}, \end{aligned} \quad (21)$$

where  $x_i(t)$  denotes the augmented state vector of  $\Sigma_i^{DG}$ , defined as

$$x_i \triangleq [V_i^d \quad V_i^q \quad I_{ti}^d \quad I_{ti}^q \quad v_i^d \quad v_i^q \quad \tilde{\omega}_i]^\top, \quad (22)$$

(the augmented local state component  $\tilde{\omega}_i$  will be formally introduced in the sequel, but it is not required here for local controllers),  $K_{i0} = [K_i^P \quad \mathbf{0}_{2 \times 2} \quad K_i^I \quad \mathbf{0}_{2 \times 1}] \in \mathbb{R}^{2 \times 7}$  is the local controller gain, and  $K_i^P$  and  $K_i^I$  are respectively the proportional and integral gain matrices of the local PI controllers.

Essentially, the local control input component  $u_{iL}(t)$  of the total control input  $u_i^V(t) \triangleq [V_{ti}^d(t) \quad V_{ti}^q(t)]^\top$  at the VSC of  $\Sigma_i^{DG}$  is given by:

$$u_{iL}(t) = K_i^P \begin{bmatrix} V_i^d - V_{i,ref}^d \\ V_i^q - V_{i,ref}^q \end{bmatrix} + K_i^I \begin{bmatrix} v_i^d \\ v_i^q \end{bmatrix}. \quad (23)$$

This local control architecture provides feedback from all augmented states to both  $d$ -axis and  $q$ -axis voltage control commands, enabling cross-coupling between  $d$  and  $q$  control channels when necessary for stability and performance.

### B. Distributed Controllers for Frequency Synchronization

In islanded AC MG operation, each  $\Sigma_i^{DG}$  must generate a local frequency reference  $\omega_i(t)$  for proper  $dq$ -frame transformation and system synchronization. The phase angle  $\theta_i(t)$  required for the Park transformation is obtained through:

$$\theta_i(t) = \int_0^t \omega_i(\tau) d\tau. \quad (24)$$

To maintain frequency coherence while preserving droop-free power-sharing characteristics, we incorporate frequency dynamics via normalized power consensus [24]. However, directly implementing an algebraic relationship

$$\omega_i(t) = \omega_0 + u_i^\Omega(t),$$

with a distributed consensus control input

$$u_i^\Omega(t) = \sum_{j \in \mathcal{N}_i^C} K_{ij}^\Omega (P_{n,i}(t) - P_{n,j}(t)), \quad (25)$$

(where  $P_{n,i}(t) = P_i(t)/P_i^{\max}$  represents normalized active power injection from  $\Sigma_i^{DG}$ ) would create an implicit system unsuitable for state-space analysis. Therefore, we model the frequency dynamics using a first-order filter that captures

realistic measurement, communication, and actuation delays:

$$\tau_i \frac{d\omega_i(t)}{dt} = -\omega_i(t) + \omega_0 + u_i^\Omega(t), \quad (26)$$

where  $\tau_i > 0$  is a small time constant representing the combined effect of sensing, communication, and control delays in the frequency control loop. To obtain frequency error dynamics, we define  $\tilde{\omega}_i = \omega_i - \omega_0$ , which yields:

$$\tau_i \frac{d\tilde{\omega}_i(t)}{dt} = -\tilde{\omega}_i + u_i^\Omega(t). \quad (27)$$

The used distributed consensus control input  $u_i^\Omega(t)$  ensures that frequency deviations are directly proportional to normalized power imbalances among communicating DGs. When all DGs reach normalized power consensus, the system frequency converges to the nominal value  $\omega_0$ , achieving both proportional power sharing and frequency synchronization objectives without compromising the droop-free operation principle. More details on the used distributed controllers are discussed in the following subsection.

### C. Distributed Controllers for Proportional Power Sharing

While the local controllers ensure voltage regulation, they do not address proportional power sharing among DGs. To achieve proportional power sharing, we use distributed global controllers that leverage communication networks (droop-free) to eliminate the need for centralized coordination.

The distributed control strategy employs consensus-based algorithms to achieve proportional sharing of active and reactive power among DGs. For each  $\Sigma_i^{DG}$ , the distributed control laws are:

$$\begin{aligned} u_i^P(t) &= \sum_{j \in \mathcal{N}_i^C} K_{ij}^P (P_{i,n}(t) - P_{j,n}(t)), \\ u_i^Q(t) &= \sum_{j \in \mathcal{N}_i^C} K_{ij}^Q (Q_{i,n}(t) - Q_{j,n}(t)), \end{aligned} \quad (28)$$

where  $K_{ij}^P$  and  $K_{ij}^Q$  are the active and reactive power sharing distributed controller gains, and  $P_{i,n}(t) = P_i(t)/P_i^{\max}$  and  $Q_{i,n}(t) = Q_i(t)/Q_i^{\max}$  are the normalized active and reactive power values with  $P_i^{\max}$  and  $Q_i^{\max}$  being the maximum power ratings of  $\Sigma_i^{DG}$ . Recall that the active and reactive power measurements  $P_i(t)$  and  $Q_i(t)$  at each DG  $\Sigma_i^{DG}$  can be obtained via (9).

The overall VSC control input  $u_i^V(t) \triangleq [V_{ti}^d(t) \ V_{ti}^q(t)]^\top$  combines local steady-state controllers, local feedback controllers and global distributed controllers:

$$u_i^V(t) \triangleq \begin{bmatrix} V_{ti}^d(t) \\ V_{ti}^q(t) \end{bmatrix} = u_{iS} + u_{iL}(t) + u_{iG}(t), \quad (29)$$

where  $u_{iG}(t) = [u_i^P(t) \ u_i^Q(t)]^\top$  represents the distributed controller (28),  $u_{iL}(t)$  is the local controller (21), and  $u_{iS}$  is the steady-state controller (to be designed in the sequel).

It is worth noting that we can restate (29) in *dq* frame as

$$u_i^{Vdq}(t) \triangleq V_{ti}^{dq}(t) = u_{iS}^{dq} + u_{iL}^{dq}(t) + u_{iG}^{dq}(t). \quad (30)$$

This droop-free approach eliminates the traditional trade-off between voltage regulation and power sharing accuracy by directly coordinating through communication rather than relying on local droop characteristics.

### D. Closed-Loop Dynamics of the AC MG

By combining (7), (20) and (27), the overall dynamics of  $\Sigma_i^{DG}$ ,  $i \in \mathbb{N}_N$  can be written as:

$$\frac{dV_i^{dq}}{dt} = -i(\omega_0 + \tilde{\omega}_i)V_i^{dq} + \frac{I_{ti}^{dq}}{C_{ti}} - \frac{I_{Li}^{dq}}{C_{ti}} - \frac{I_i^{dq}}{C_{ti}} + w_{vi}^{dq}(t), \quad (31a)$$

$$\frac{dI_{ti}^{dq}}{dt} = -\frac{V_i^{dq}}{L_{ti}} - \left( \frac{R_{ti}}{L_{ti}} + i(\omega_0 + \tilde{\omega}_i) \right) I_{ti}^{dq} + \frac{u_i^{Vdq}}{L_{ti}} + w_{ci}^{dq}(t), \quad (31b)$$

$$\frac{dv_i^{dq}}{dt} = V_i^{dq} - V_{i,ref}^{dq}, \quad (31c)$$

$$\frac{d\tilde{\omega}_i}{dt} = -\frac{1}{\tau_i} \tilde{\omega}_i + \frac{1}{\tau_i} u_i^\Omega, \quad (31d)$$

where the terms  $I_i^{dq}$ ,  $I_{Li}^{dq}$ ,  $u_i^{Vdq}$ , and  $u_i^\Omega$  can all be substituted from (8), (10), (30) and (25), respectively, and  $w_{vi}^{dq}(t)$  and  $w_{ci}^{dq}$  are unknown zero-mean disturbances (accounting for model uncertainties and external impacts). Using the commonly adopted assumption  $P_{Li}^{dq} = 0$  (for (10)), the dynamics of  $\Sigma_i^{DG}$  (31) can be written in compact state-space form as:

$$\dot{x}_i(t) = A_i x_i(t) + B_i u_i(t) + E_i d_i(t) + F_i \xi_i(t) + g_i(x_i(t)), \quad (32)$$

where  $x_i(t)$  is the state vector as defined in (22),  $u_i(t) \triangleq [u_i^V(t) \ u_i^\Omega(t)]^\top$  is the total control input,  $d_i(t)$  is the exogenous input (disturbance) defined as:

$$d_i(t) \triangleq \bar{w}_i + w_i(t), \quad (33)$$

with  $\bar{w}_i \triangleq [-\bar{I}_{Li}^d \ -\bar{I}_{Li}^q \ 0 \ 0 \ -V_{i,ref}^d \ -V_{i,ref}^q \ 0]^\top$  representing the known fixed (mean) disturbance and  $w_i(t) = [w_{vi}^d(t) \ w_{vi}^q(t) \ w_{ci}^d(t) \ w_{ci}^q(t) \ 0 \ 0]^\top$  representing the unknown zero-mean disturbance,

$$\xi_i(t) \triangleq [I_i^d \ I_i^q]^\top \quad (34)$$

is the distribution line coupling input (recall  $I_i^{dq} = \sum_{l \in \mathcal{E}_i} \mathcal{B}_{il} I_l^{dq}(t)$ ), and

$$g_i(x_i(t)) \triangleq [-\tilde{\omega}_i V_i^q \ -\tilde{\omega}_i V_i^d \ -\tilde{\omega}_i I_{ti}^q \ -\tilde{\omega}_i I_{ti}^d \ 0 \ 0]^\top, \quad (35)$$

captures the nonlinear coupling terms.

In (32), the system matrix  $A_i$ , control input matrix  $B_i$ , disturbance input matrix  $E_i$ , and distribution line coupling

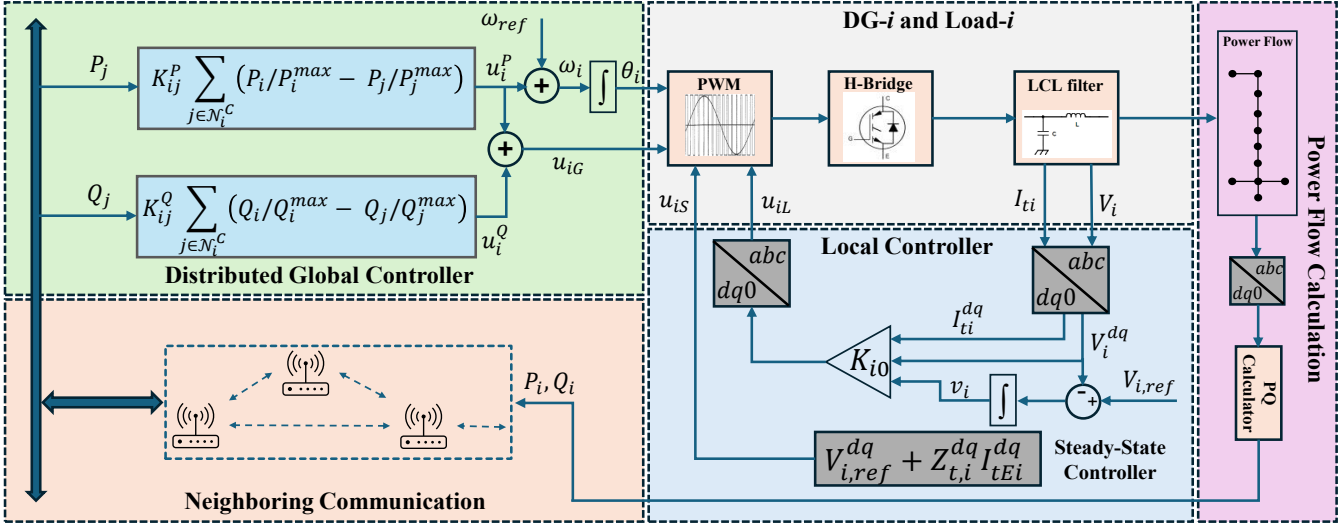


Fig. 4. Hierarchical control architecture combining local and distributed controllers through physical and communication interconnections.

matrix  $F_i$  are given respectively by:

$$\begin{aligned}
 A_i &\triangleq \begin{bmatrix} -\frac{Y_{L,i}}{C_{ti}} & \omega_0 & \frac{1}{C_{ti}} & 0 & 0 & 0 & 0 \\ -\omega_0 & -\frac{Y_{L,i}}{C_{ti}} & 0 & \frac{1}{C_{ti}} & 0 & 0 & 0 \\ -\frac{1}{L_{ti}} & 0 & -\frac{R_{ti}}{L_{ti}} & \omega_0 & 0 & 0 & 0 \\ 0 & -\frac{1}{L_{ti}} & -\omega_0 & -\frac{R_{ti}}{L_{ti}} & 0 & 0 & 0 \\ 1 & 0 & 0 & 0 & 0 & 0 & 0 \\ 0 & 1 & 0 & 0 & 0 & 0 & 0 \\ 0 & 0 & 0 & 0 & 0 & 0 & -\frac{1}{\tau_i} \end{bmatrix}, \\
 B_i &\triangleq \begin{bmatrix} 0 & 0 & \frac{1}{L_{ti}} & 0 & 0 & 0 & 0 \\ 0 & 0 & 0 & \frac{1}{L_{ti}} & 0 & 0 & 0 \\ 0 & 0 & 0 & 0 & 0 & 0 & \frac{1}{\tau_i} \end{bmatrix}^\top, \\
 E_i &\triangleq \text{diag}([C_{ti}^{-1} \ C_{ti}^{-1} \ L_{ti}^{-1} \ L_{ti}^{-1} \ 1 \ 1 \ \tau_i^{-1}]), \\
 F_i &\triangleq \begin{bmatrix} -\frac{1}{C_{ti}} & 0 & 0 & 0 & 0 & 0 & 0 \\ 0 & -\frac{1}{C_{ti}} & 0 & 0 & 0 & 0 & 0 \end{bmatrix}^\top. \tag{36}
 \end{aligned}$$

### E. Networked System Representation

This subsection formulates the closed-loop AC MG as a networked system by establishing the interconnection relationships among DGs, lines, and loads through a static interconnection matrix. We analyze each subsystem type systematically to identify its coupling mechanisms, then construct the aggregate interconnection relationship. Figure 5 illustrates the identified overall networked system representation of the AC MG.

1) **DG Subsystems:** Note that each DG control input  $u_i(t)$  in (32) can be expressed as

$$u_i(t) = \begin{bmatrix} u_i^V(t) \\ u_i^\Omega(t) \end{bmatrix} = \begin{bmatrix} \mathbf{I}_{2 \times 2} \\ \mathbf{0}_{1 \times 2} \end{bmatrix} (u_{iS} + u_{iL}(t)) + u_i^D(t),$$

where  $u_{iS}$  is the steady-state controller,  $u_{iL}(t)$  is the local feedback controller that takes the form (21):

$$u_{iL}(t) = K_{i0} x_i(t) - K_i^P \begin{bmatrix} V_{i,ref}^d \\ V_{i,ref}^q \end{bmatrix},$$

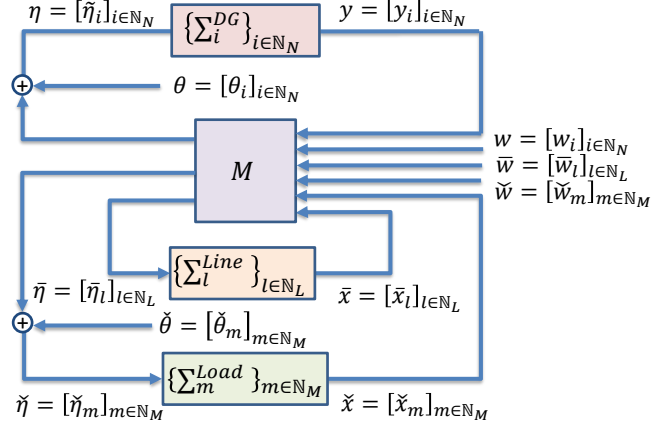


Fig. 5. Networked system representation showing interconnections between DGs, lines, and loads AC MG.

and  $u_i^D(t)$  is the global distributed controller that takes the form (by combining (25), (28)):

$$\begin{aligned}
 u_i^D(t) &\triangleq \begin{bmatrix} u_i^G(t) \\ u_i^\Omega(t) \end{bmatrix} = \begin{bmatrix} u_i^P(t) \\ u_i^Q(t) \\ u_i^\Omega(t) \end{bmatrix} \\
 &= \sum_{j \in \mathcal{N}_i^C} \underbrace{\begin{bmatrix} K_{ij}^P & \mathbf{0} \\ \mathbf{0} & K_{ij}^Q \\ K_{ij}^\Omega & \mathbf{0} \end{bmatrix}}_{\triangleq \bar{K}_{ij}} \begin{bmatrix} P_{i,n}(t) - P_{j,n}(t) \\ Q_{i,n}(t) - Q_{j,n}(t) \end{bmatrix} \\
 &= \sum_{j \in \mathcal{N}_i^C} \hat{K}_{ij} \begin{bmatrix} P_j(t) \\ Q_j(t) \end{bmatrix}, \tag{37}
 \end{aligned}$$

where we define  $\bar{\mathcal{N}}_i^C \triangleq \mathcal{N}_i^C \cup \{i\}$ , and

$$\hat{K}_{ij} \triangleq \begin{cases} -\bar{K}_{ij} \begin{bmatrix} P_j^{\max} & \mathbf{0} \\ \mathbf{0} & Q_j^{\max} \end{bmatrix}^{-1}, & j \in \mathcal{N}_i^C, \\ \sum_{j \in \mathcal{N}_i^C} \bar{K}_{ij} \begin{bmatrix} P_i^{\max} & \mathbf{0} \\ \mathbf{0} & Q_i^{\max} \end{bmatrix}^{-1}, & j = i. \end{cases} \tag{38}$$

It is worth noting that, when designing  $\hat{K}_{ij}$  blocks, to uniquely obtain the corresponding distributed controller gain matrices  $K_{ij}^P$ ,  $K_{ij}^Q$ , and  $K_{ij}^{\Omega}$ , we have to embed two structural constraints: (i) each off-diagonal  $\hat{K}_{ij}$  block (i.e.,  $j \neq i$ ) should be structured similarly to the corresponding  $\bar{K}_{ij}$  block (i.e., with three inner  $\mathbf{0}$  blocks, see (37)); and (ii) each diagonal  $\hat{K}_{ii}$  block (i.e.,  $\hat{K}_{ii}$ ) should satisfy

$$\hat{K}_{ii} = - \sum_{j \in \mathcal{N}_i^C} \hat{K}_{ij} \begin{bmatrix} P_j^{\max} & \mathbf{0} \\ 0 & Q_j^{\max} \end{bmatrix} \begin{bmatrix} P_i^{\max} & \mathbf{0} \\ 0 & Q_i^{\max} \end{bmatrix}^{-1}. \quad (39)$$

Applying this  $u_i(t)$  form in (32), we can obtain the closed-loop dynamics of each DG subsystem  $\Sigma_i^{DG}$ ,  $i \in \mathbb{N}_N$  as:

$$\dot{x}_i(t) = \hat{A}_i x_i(t) + \hat{B}_i \eta_i(t) + g_i(x_i(t)) + \theta_i, \quad (40)$$

where  $\hat{A}_i \triangleq A_i + \bar{B}_i K_{i0}$ ,  $\bar{B}_i \triangleq B_i [\mathbf{I}_{2 \times 2} \quad \mathbf{0}_{2 \times 1}]^\top$ , and  $\hat{B}_i \triangleq [B_i \quad F_i \quad E_i]$ . In (40),  $g_i(x_i)$  represents the frequency coupling nonlinearity defined in (35),  $\theta_i$  represents the effective steady-state input that takes the form:

$$\theta_i \triangleq \bar{B}_i (u_{iS} - K_i^P \begin{bmatrix} V_{i,ref}^d \\ V_{i,ref}^q \end{bmatrix}) + E_i \bar{w}_i,$$

and  $\eta_i(t)$  represents the effective control input, defined as

$$\eta_i(t) \triangleq \begin{bmatrix} u_i^D(t) \\ \xi_i(t) \\ w_i(t) \end{bmatrix}, \quad (41)$$

where  $u_i^D(t)$  is the distributed control input (through the communication topology),  $\xi_i(t)$  is the distribution line coupling input that takes the form:

$$\xi_i = \begin{bmatrix} I_i^d \\ I_i^q \end{bmatrix} = \sum_{l \in \mathcal{E}_i} \mathcal{B}_{il} \begin{bmatrix} I_l^d \\ I_l^q \end{bmatrix} = \sum_{l \in \mathcal{E}_i} \bar{C}_{il} \bar{x}_l, \quad (42)$$

where  $\bar{C}_{il} \triangleq \mathcal{B}_{il} \mathbf{I}_2$ , and  $w_i(t)$  represents the unknown zero-mean disturbances from (33).

Since the injected active and reactive power (from power flow equations (9)) and PCC voltage of each DG impact other elements in the AC MG, we define an output vector  $y_i$  for each  $\Sigma_i^{DG}$  as:

$$y_i \triangleq [V_i^d \quad V_i^q \quad P_i \quad Q_i]^\top = h_i(x_i, \eta_i). \quad (43)$$

The first two components  $V_i^d$  and  $V_i^q$  of the output  $y_i$  are the first two components of the DG state  $x_i$  in (40). These DG output components affect the physically connected line dynamics (17) via (18), as they determine the line inputs as:

$$\bar{u}_l = \sum_{k \in \mathcal{N}_l^P} \mathcal{B}_{kl} \begin{bmatrix} V_k^d \\ V_k^q \end{bmatrix} = \sum_{k \in \mathcal{N}_l^P} C_{lk} y_k,$$

where  $C_{lk} \triangleq \mathcal{B}_{kl} [\mathbf{I}_2 \quad \mathbf{0}_{2 \times 2}] = [\mathcal{B}_{kl} \mathbf{I}_2 \quad \mathbf{0}_{2 \times 2}]$ . On the other hand, the last two components  $P_i$  and  $Q_i$  of the output  $y_i$  can be computed via (9) using DG state components  $V_i^d$ ,  $V_i^q$  and DG input component  $\xi_i$  in (40). These DG output components affect the dynamics of neighboring DGs (40) via (37), as they determine the distributed control input as

$$u_i^D = \sum_{j \in \mathcal{N}_i^C} \hat{K}_{ij} \begin{bmatrix} P_j \\ Q_j \end{bmatrix} = \sum_{j \in \mathcal{N}_i^C} K_{ij} y_j,$$

where  $K_{ij} \triangleq \hat{K}_{ij} [\mathbf{0}_{2 \times 2} \quad \mathbf{I}_2] = [\mathbf{0}_{3 \times 2} \quad \hat{K}_{ij}]$ . Conse-

quently, we can express  $\eta_i(t)$  as

$$\eta_i(t) \triangleq \begin{bmatrix} u_i^D(t) \\ \xi_i(t) \\ w_i(t) \end{bmatrix} = \begin{bmatrix} \sum_{j \in \mathcal{N}_i^C} K_{ij} y_j(t) \\ \sum_{l \in \mathcal{E}_i} \bar{C}_{il} \bar{x}_l(t) \\ w_i(t) \end{bmatrix}. \quad (44)$$

2) **Line Subsystems:** Each distribution line subsystem  $\Sigma_l^{Line}$ ,  $l \in \mathbb{N}_L$  follows the dynamics from (17):

$$\dot{x}_l(t) = \bar{A}_l \bar{x}_l(t) + \hat{B}_l \bar{\eta}_l(t), \quad (45)$$

where

$$\hat{B}_l \triangleq [\bar{B}_l \quad \bar{B}_l \quad \bar{E}_l], \quad (46)$$

with  $\bar{B}_l$  as defined in (19), and  $\bar{E}_l \triangleq (1/L_l) \mathbf{I}_2$ . In (45),  $\bar{\eta}_l$  represents the effective input (driven mainly by the applied voltage difference by the connected DGs and Loads) that takes the form:

$$\bar{\eta}_l(t) = \begin{bmatrix} \sum_{k \in \mathcal{N}_l^P} C_{lk} y_k(t) \\ \sum_{m \in \mathcal{N}_l^P} \check{C}_{lm} \check{x}_m(t) \\ \bar{w}_l(t) \end{bmatrix}, \quad (47)$$

where

$$C_{lk} \triangleq \mathcal{B}_{kl} [\mathbf{I}_2 \quad \mathbf{0}_{2 \times 2}] = [\mathcal{B}_{kl} \mathbf{I}_2 \quad \mathbf{0}_{2 \times 2}], \quad (48)$$

$$\check{C}_{lm} \triangleq \mathcal{B}_{ml} \mathbf{I}_2, \quad (49)$$

and  $\bar{w}_l(t)$  represents an unknown zero-mean disturbance (added on to (17)) to account for model uncertainties.

3) **Load Subsystems:** Each load subsystem  $\Sigma_m^{Load}$ ,  $m \in \mathbb{N}_M$  follows dynamics from (14):

$$\dot{x}_m(t) = \check{A}_m \check{x}_m(t) + \hat{B}_m \check{\eta}_m(t) + \check{\theta}_m(t), \quad (50)$$

where

$$\hat{B}_m \triangleq [\check{B}_m \quad \check{E}_m], \quad (51)$$

with  $\check{B}_m$  as defined in (15) and  $\check{E}_m \triangleq \check{B}_m$ . In (50),  $\check{\theta}_m$  represents the steady-state input that takes the form  $\check{\theta}_m \triangleq \check{B}_m \check{d}_m$ ,  $\check{\eta}_m(t)$  represents the effective input (driven mainly by currents injected from connected lines) that takes the form:

$$\check{\eta}_m(t) \triangleq \begin{bmatrix} \sum_{l \in \mathcal{E}_m} \check{C}_{ml} \bar{x}_l(t) \\ \check{w}_m(t) \end{bmatrix}, \quad (52)$$

where

$$\check{C}_{ml} \triangleq \mathcal{B}_{ml} \mathbf{I}_2, \quad (53)$$

and  $\check{w}_m(t)$  represents an unknown zero-mean disturbance (added on to (14)) to account for model uncertainties.

4) **Networked System Representation:** We now construct the networked system representation by vectorizing the identified subsystem dynamics. For DG subsystems, vectorizing (40), (43) and (44) yields:

$$\begin{cases} \dot{x}(t) = \hat{A}x(t) + \hat{B}\eta(t) + G(x(t)) + \theta, \\ y(t) = H(x(t), \eta(t)), \\ \eta(t) = Ky(t) + \bar{C}\bar{x}(t) + Ew(t), \end{cases} \quad (54)$$

where we define the vectors:  $x \triangleq [x_i^\top]_{i \in \mathbb{N}_N}^\top$ ,  $\eta \triangleq [\eta_i^\top]_{i \in \mathbb{N}_N}^\top$ ,  $\theta \triangleq [\theta_i^\top]_{i \in \mathbb{N}_N}^\top$ ,  $y \triangleq [y_i^\top]_{i \in \mathbb{N}_N}^\top$ ,  $\bar{x} \triangleq [\bar{x}_l^\top]_{l \in \mathbb{N}_L}^\top$ ,  $w \triangleq [w_i^\top]_{i \in \mathbb{N}_N}^\top$ , the matrices:  $\hat{A} \triangleq \text{diag}([\hat{A}_i]_{i \in \mathbb{N}_N})$ ,  $\hat{B} \triangleq$

$$\text{diag}([\hat{B}_i]_{i \in \mathbb{N}_N}),$$

$$K \triangleq \begin{bmatrix} K_{ij} \\ \mathbf{0} \\ \mathbf{0} \end{bmatrix}_{i,j \in \mathbb{N}_N}, \quad \bar{C} \triangleq \begin{bmatrix} \mathbf{0} \\ \bar{C}_{il} \\ \mathbf{0} \end{bmatrix}_{i \in \mathbb{N}_N, l \in \mathbb{N}_L},$$

$$E \triangleq \text{diag} \left( \begin{bmatrix} \mathbf{0} \\ \mathbf{0} \\ \mathbf{I} \end{bmatrix}_{i \in \mathbb{N}_N} \right),$$

and the vector spaces:

$$G(x) \triangleq [g_i^\top(x_i)]_{i \in \mathbb{N}_N}^\top, \quad H(x) \triangleq [h_i^\top(x_i, \eta_i)]_{i \in \mathbb{N}_N}^\top.$$

For line subsystems, vectorizing (45) and (47) yields:

$$\begin{cases} \dot{\bar{x}}(t) = \bar{A}\bar{x}(t) + \bar{B}\bar{\eta}(t), \\ \bar{\eta}(t) = Cx(t) + \bar{C}\bar{x}(t) + \bar{E}\bar{w}(t), \end{cases} \quad (55)$$

where we define the vectors  $\bar{\eta} \triangleq [\bar{\eta}_l^\top]_{l \in \mathbb{N}_L}^\top$ ,  $\bar{x} \triangleq [\bar{x}_m^\top]_{m \in \mathbb{N}_M}^\top$ ,  $\bar{w} \triangleq [\bar{w}_l^\top]_{l \in \mathbb{N}_L}^\top$ , and the matrices  $\bar{A} \triangleq \text{diag}([\bar{A}_l]_{l \in \mathbb{N}_L})$ ,  $\bar{B} \triangleq \text{diag}([\bar{B}_l]_{l \in \mathbb{N}_L})$ ,

$$\begin{aligned} C \triangleq & \begin{bmatrix} C_{lk} \\ \mathbf{0} \\ \mathbf{0} \end{bmatrix}_{l \in \mathbb{N}_L, k \in \mathbb{N}_N}, \quad \bar{C} \triangleq \begin{bmatrix} \mathbf{0} \\ \bar{C}_{lm} \\ \mathbf{0} \end{bmatrix}_{l \in \mathbb{N}_L, m \in \mathbb{N}_M}, \\ \bar{E} \triangleq & \text{diag} \left( \begin{bmatrix} \mathbf{0} \\ \mathbf{0} \\ \mathbf{I} \end{bmatrix}_{l \in \mathbb{N}_L} \right). \end{aligned}$$

For load subsystems, vectorizing (50) and (52) yields:

$$\begin{cases} \dot{\check{x}}(t) = \check{A}\check{x}(t) + \hat{B}\check{\eta}(t) + \check{\theta}, \\ \check{\eta}(t) = \check{C}\check{x}(t) + \check{E}\check{w}(t), \end{cases} \quad (56)$$

where we define the vectors  $\check{\eta} \triangleq [\check{\eta}_m^\top]_{m \in \mathbb{N}_M}^\top$ ,  $\check{w} \triangleq [\check{w}_m^\top]_{m \in \mathbb{N}_M}^\top$ , and  $\check{\theta} \triangleq [\check{\theta}_m^\top]_{m \in \mathbb{N}_M}^\top$ , and the matrices:  $\check{A} \triangleq \text{diag}([\check{A}_m]_{m \in \mathbb{N}_M})$ ,  $\hat{B} \triangleq \text{diag}([\hat{B}_m]_{m \in \mathbb{N}_M})$ ,

$$\check{C} = \begin{bmatrix} \check{C}_{ml} \\ \mathbf{0} \end{bmatrix}_{m \in \mathbb{N}_M, l \in \mathbb{N}_L}, \quad \check{E} = \text{diag} \left( \begin{bmatrix} \mathbf{0} \\ \mathbf{I} \end{bmatrix}_{m \in \mathbb{N}_M} \right).$$

The interconnection relationship among DGs (54), Lines (55) and Loads (56), as shown in Fig. 5, now can be identified as:

$$\begin{bmatrix} \eta \\ \bar{\eta} \\ \check{\eta} \end{bmatrix} = \underbrace{\begin{bmatrix} K & \bar{C} & \mathbf{0} & E & \mathbf{0} & \mathbf{0} \\ C & \mathbf{0} & \check{C} & \mathbf{0} & \bar{E} & \mathbf{0} \\ \mathbf{0} & \check{C} & \mathbf{0} & \mathbf{0} & \mathbf{0} & \check{E} \end{bmatrix}}_{\triangleq M} \begin{bmatrix} y \\ \bar{x} \\ \check{x} \\ w \\ \bar{w} \\ \check{w} \end{bmatrix}, \quad (57)$$

where  $M$  is the interconnection matrix.

## V. NETWORKED SYSTEM ERROR DYNAMICS AND EQUILIBRIUM POINT ANALYSIS

This section analyzes the equilibrium point of the closed-loop AC MG system and derives the networked system error dynamics. This equilibrium point analysis enables the design of steady-state control to simultaneously achieve voltage regulation, frequency synchronization, and proportional power sharing objectives at steady state (equilibrium). To conduct this equilibrium point analysis, we start by formulating the

error dynamics by defining ‘error variables’ (denoted with  $\tilde{\cdot}$ , e.g.,  $\tilde{V}_i^{dq}$ ) as deviations from the identified ‘equilibrium values’ of those variables (denoted with  $\cdot_E$ , e.g.,  $V_{Ei}^{dq}$ ). This will then enable us to identify the conditions on such equilibrium variables and design the steady-state controllers such that the desired objectives are satisfied at the steady state (e.g.,  $V_{Ei}^{dq} = V_{i,ref}^{dq}$ ). Subsequently, this framework will also enable us to co-design the feedback controllers and topology to ensure the closed-loop stability and performance of the AC MG system using the dissipativity-based co-design ideas given in Sec. II (e.g., to provide  $\lim_{t \rightarrow \infty} \tilde{V}_i^{dq}(t) = V_{Ei}^{ref}$ ).

### A. Formulating Networked System Error Dynamics

To analyze the closed-loop AC MG around an equilibrium point, we define error variables as deviations from constant equilibrium states of those variables. For the DG, line, and load subsystems, we define the error variables as:

$$\tilde{V}_i^{dq} \triangleq V_i^{dq} - V_{Ei}^{dq}, \quad (58a)$$

$$\tilde{I}_{ti}^{dq} \triangleq I_{ti}^{dq} - I_{tEi}^{dq}, \quad (58b)$$

$$\tilde{v}_i^{dq} \triangleq v_i^{dq} - v_{Ei}^{dq}, \quad (58c)$$

$$\tilde{I}_i^{dq} \triangleq I_i^{dq} - I_{Ei}^{dq}, \quad (58d)$$

$$\tilde{I}_l^{dq} \triangleq I_l^{dq} - I_{El}^{dq}, \quad (58e)$$

$$\tilde{V}_m^{dq} \triangleq V_m^{dq} - V_{Em}^{dq}, \quad (58f)$$

where we require  $V_{Ei}^{dq} = V_{i,ref}^{dq}$  and  $v_{Ei}^{dq} = 0$  due to the voltage regulation objective. For the frequency error state  $\tilde{\omega}_i$  defined in (27), its equilibrium state value is by definition  $\tilde{\omega}_{Ei} \triangleq 0$  due to the frequency synchronization objective.

At equilibrium, all time derivatives of states vanish, i.e.,  $\dot{x}_{Ei} = 0$ ,  $\dot{\bar{x}}_{El} = 0$ ,  $\dot{\check{x}}_{Em} = 0$ ,  $\forall i, l, m$ . Since the error states of DGs, lines, and loads are defined such that:

$\tilde{x}_i \triangleq x_i - x_{Ei}$ ,  $\tilde{x}_l \triangleq \bar{x}_l - \bar{x}_{El}$ ,  $\tilde{x}_m \triangleq \check{x}_m - \check{x}_{Em}$ ,  $\forall i, l, m$ , their time derivatives are equal to those of the original states:

$$\dot{\tilde{x}}_i = \dot{x}_i, \quad \dot{\tilde{x}}_l = \dot{\bar{x}}_l, \quad \dot{\tilde{x}}_m = \dot{\check{x}}_m, \quad \forall i, l, m.$$

Therefore, error dynamics can be derived by substituting original variables with error variables (and equilibrium point variables) in the closed-loop dynamics.

1) **DG Error Subsystems:** For example, we substitute  $x_i = \tilde{x}_i + x_{Ei}$  and  $\eta_i = \tilde{\eta}_i + \eta_{Ei}$  into the closed-loop DG dynamics (40) to obtain:

$$\dot{\tilde{x}}_i = \hat{A}_i(\tilde{x}_i + x_{Ei}) + \hat{B}_i(\tilde{\eta}_i + \eta_{Ei}) + g_i(\tilde{x}_i + x_{Ei}) + \theta_i. \quad (59)$$

From the structure of the frequency coupling nonlinearity  $g_i(\cdot)$  (35), it can be shown that  $g_i(\tilde{x}_i + x_{Ei}) = g_i(\tilde{x}_i) + \bar{g}_i(x_{Ei})\tilde{\omega}_i = g_i(\tilde{x}_i) + \bar{g}_i(x_{Ei})e_7^\top \tilde{x}_i$  where  $\bar{g}_i(x_{Ei}) \triangleq [-V_{Ei}^q \quad -V_{Ei}^d \quad -I_{tEi}^q \quad -I_{tEi}^d \quad 0 \quad 0 \quad 0]^\top$  and  $e_7$  is the unit vector in  $\mathbb{R}^{7 \times 1}$  with a 1 in the last element. Therefore, by expanding (59) and grouping terms by error and equilibrium components, we can simplify the DG error dynamics as:

$$\dot{\tilde{x}}_i = \tilde{A}_i\tilde{x}_i + \hat{B}_i\tilde{\eta}_i + g_i(\tilde{x}_i) + (\hat{A}_i x_{Ei} + \hat{B}_i \eta_{Ei} + \theta_i).$$

where  $\tilde{A}_i \triangleq (\hat{A}_i + \bar{g}_i(x_{Ei})e_7^\top)$ . This implies that, to avoid steady-state errors at the equilibrium point, we require:

$$\hat{A}_i x_{Ei} + \hat{B}_i \eta_{Ei} + \theta_i = 0. \quad (60)$$

To ensure that this condition holds, we leverage the tunable steady-state control input term  $u_{iS}$  inside  $\theta_i$ . Under this condition (60), the DG error dynamics simplify to:

$$\dot{\tilde{x}}_i = \tilde{A}_i \tilde{x}_i + \tilde{B}_i \tilde{\eta}_i + g_i(\tilde{x}_i). \quad (61)$$

In (61), the DG input error  $\tilde{\eta}_i$  is formally defined as:

$$\begin{aligned} \tilde{\eta}_i &\triangleq \eta_i - \eta_{Ei} = \begin{bmatrix} u_i^D(t) - u_{Ei}^D \\ \xi_i(t) - \xi_{Ei} \\ w_i(t) - w_{Ei} \end{bmatrix} = \begin{bmatrix} u_i^D(t) \\ \xi_i(t) - \xi_{Ei} \\ w_i(t) \end{bmatrix} \\ &= \begin{bmatrix} \sum_{j \in \mathcal{N}_i^C} K_{ij} \tilde{y}_j(t) \\ \sum_{l \in \mathcal{E}_i} \tilde{C}_{il} \tilde{x}_l(t) \\ w_i(t) \end{bmatrix}, \end{aligned} \quad (62)$$

where  $\eta_{Ei}$  is the DG input at the equilibrium, consisting of three components: (i) distributed control input (37) at the equilibrium  $u_{Ei}^D = \mathbf{0}$  (due to power consensus), line coupling input (34) at the equilibrium  $\xi_{Ei}$  (non-zero in general), and (iii) disturbance at the equilibrium  $w_{Ei} = \mathbf{0}$  (as disturbance is zero-mean). On the other hand, in (61), frequency coupling nonlinearity error  $g_i(\tilde{x}_i)$  takes the form (identically to (35))

$$g_i(\tilde{x}_i) \triangleq [-\tilde{\omega}_i \tilde{V}_i^q \quad -\tilde{\omega}_i \tilde{V}_i^d \quad -\tilde{\omega}_i \tilde{I}_{ti}^q \quad -\tilde{\omega}_i \tilde{I}_{ti}^d \quad 0 \quad 0 \quad 0]^\top. \quad (63)$$

The DG output error  $\tilde{y}_i$  is formally defined (and simplified using (43)) as:

$$\begin{aligned} \tilde{y}_i &\triangleq y_i - y_{Ei} = h_i(x_i, \eta_i) - h_i(x_{Ei}, \eta_{Ei}) \\ &= [\tilde{V}_i^d \quad \tilde{V}_i^q \quad \tilde{P}_i \quad \tilde{Q}_i], \end{aligned} \quad (64)$$

where the power errors  $\tilde{P}_i, \tilde{Q}_i$  can be linearized around the operating (equilibrium) point  $(x_{Ei}, \eta_{Ei})$  (using (9)) to obtain the approximations:

$$\begin{aligned} \tilde{P}_i &\triangleq P_i - P_{Ei} \approx V_{Ei}^d \tilde{I}_i^d + I_{Ei}^d \tilde{V}_i^d + V_{Ei}^q \tilde{I}_i^q + I_{Ei}^q \tilde{V}_i^q, \\ \tilde{Q}_i &\triangleq Q_i - Q_{Ei} \approx V_{Ei}^q \tilde{I}_i^d - V_{Ei}^d \tilde{I}_i^q + I_{Ei}^d \tilde{V}_i^q - I_{Ei}^q \tilde{V}_i^d. \end{aligned} \quad (65)$$

Consequently, DG output error  $\tilde{y}_i$  can be expressed as:

$$\tilde{y}_i = C_i^y \tilde{x}_i + D_i^y \tilde{\eta}_i, \quad (66)$$

where

$$\begin{aligned} C_i^y &\triangleq \begin{bmatrix} 1 & 0 & \mathbf{0}_{1 \times 5} \\ 0 & 1 & \mathbf{0}_{1 \times 5} \\ I_{Ei}^d & I_{Ei}^q & \mathbf{0}_{1 \times 5} \\ -I_{Ei}^q & I_{Ei}^d & \mathbf{0}_{1 \times 5} \end{bmatrix}, \\ D_i^y &\triangleq \begin{bmatrix} \mathbf{0}_{1 \times 3} & 0 & 0 & \mathbf{0}_{1 \times 7} \\ \mathbf{0}_{1 \times 3} & 0 & 0 & \mathbf{0}_{1 \times 7} \\ \mathbf{0}_{1 \times 3} & V_{Ei}^d & V_{Ei}^q & \mathbf{0}_{1 \times 7} \\ \mathbf{0}_{1 \times 3} & V_{Ei}^q & -V_{Ei}^d & \mathbf{0}_{1 \times 7} \end{bmatrix}. \end{aligned}$$

Essentially, the first two rows of  $C_i^y$  extract the voltage error states  $\tilde{V}_i^d, \tilde{V}_i^q$ , while the last two rows of  $C_i^y$  and  $D_i^y$  compute the linearized power outputs via (65).

2) **Line Error Subsystems:** For line subsystems, substituting  $\bar{x}_l = \tilde{x}_l + \bar{x}_{El}$  and  $\bar{\eta}_l = \tilde{\eta}_l + \bar{\eta}_{lE}$  into (45) yields:

$$\dot{\tilde{x}}_l = \bar{A}_l(\tilde{x}_l + \bar{x}_{El}) + \hat{B}_l(\tilde{\eta}_l + \bar{\eta}_{lE}).$$

At equilibrium, we require

$$\bar{A}_l \bar{x}_{El} + \hat{B}_l \bar{\eta}_{lE} = 0, \quad (67)$$

which simplifies the line error dynamics to:

$$\dot{\tilde{x}}_l = \bar{A}_l \tilde{x}_l + \hat{B}_l \tilde{\eta}_l. \quad (68)$$

In (68), the line input error  $\tilde{\eta}_l$  can be expressed as (using (47) and the fact that line disturbances  $\bar{w}_l$  are zero-mean):

$$\tilde{\eta}_l = \begin{bmatrix} \sum_{k \in \mathcal{N}_l^P \cap \mathcal{D}} C_{lk} \tilde{y}_k \\ \sum_{m \in \mathcal{N}_l^P \cap \mathcal{L}} \bar{C}_{lm} \tilde{x}_m \\ \bar{w}_l \end{bmatrix}. \quad (69)$$

3) **Load Error Subsystems:** For load subsystems, substituting  $\check{x}_m = \tilde{x} + \check{x}_{Em}$  and  $\check{\eta}_m = \tilde{\eta}_m + \check{\eta}_{mE}$  into (50) yields:

$$\dot{\check{x}}_m = \check{A}_m(\tilde{x}_m + \check{x}_{Em}) + \hat{B}_m(\tilde{\eta}_m + \check{\eta}_{mE}) + \check{\theta}_m.$$

At equilibrium, we require

$$\check{A}_m \check{x}_{Em} + \hat{B}_m \check{\eta}_{mE} + \check{\theta}_m = 0, \quad (70)$$

which simplifies the load error dynamics to:

$$\dot{\check{x}}_m = \check{A}_m \tilde{x}_m + \hat{B}_m \tilde{\eta}_m. \quad (71)$$

In (71), the load input error  $\tilde{\eta}_m$  can be expressed as (using (52) and the fact that load disturbances  $\check{w}_m$  are zero-mean):

$$\tilde{\eta}_m = \begin{bmatrix} \sum_{l \in \mathcal{E}_m} \check{C}_{ml} \tilde{x}_l \\ \check{w}_m \end{bmatrix}. \quad (72)$$

4) **Performance Outputs and Disturbance Inputs:** For dissipativity-based analysis and design of the networked system error dynamics, we have to define performance outputs for each subsystem type. For each DG error subsystem  $\tilde{\Sigma}_i^{DG}, i \in \mathbb{N}_N$ , we consider the performance output:

$$z_i(t) \triangleq H_i \tilde{y}_i(t),$$

where we select  $H_i \triangleq \mathbf{I}_4$  to motivate voltage regulation and power sharing performance. For each line error subsystem  $\tilde{\Sigma}_l^{Line}, l \in \mathbb{N}_L$ , we consider the performance output:

$$\bar{z}_l(t) \triangleq \bar{H}_l \tilde{x}_l(t),$$

where we select  $\bar{H}_l = \mathbf{I}_2$  to motivate line error (convergence) performance. For each load error subsystem  $\tilde{\Sigma}_m^{Load}, m \in \mathbb{N}_M$ , we consider the performance output:

$$\check{z}_m(t) = \check{H}_m \tilde{x}_m(t),$$

where we select  $\check{H}_m = \mathbf{I}_2$  to motivate load error (convergence) performance.

Vectorizing these performance output definitions across all subsystems yields:

$$z = H \tilde{y}, \quad \bar{z} = \bar{H} \tilde{x}, \quad \check{z} = \check{H} \tilde{x}, \quad (73)$$

where  $H \triangleq \text{diag}([H_i]_{i \in \mathbb{N}_N})$ ,  $\bar{H} \triangleq \text{diag}([\bar{H}_l]_{l \in \mathbb{N}_L})$ , and  $\check{H} \triangleq \text{diag}([\check{H}_m]_{m \in \mathbb{N}_M})$ . We consolidate the performance outputs and express them as a single vector  $z_c$ :

$$z_c \triangleq \begin{bmatrix} z \\ \bar{z} \\ \check{z} \end{bmatrix} = [H_c \quad \bar{H}_c \quad \check{H}_c] \begin{bmatrix} \tilde{y} \\ \tilde{x} \\ \tilde{x} \end{bmatrix},$$

where

$$H_c \triangleq \begin{bmatrix} H \\ \mathbf{0} \\ \mathbf{0} \end{bmatrix}, \quad \bar{H}_c \triangleq \begin{bmatrix} \mathbf{0} \\ \bar{H} \\ \mathbf{0} \end{bmatrix}, \quad \check{H}_c \triangleq \begin{bmatrix} \mathbf{0} \\ \mathbf{0} \\ \check{H} \end{bmatrix}.$$

On the other hand, we also consolidate the disturbance inputs and express them as a single vector  $w_c$ :

$$w_c \triangleq \begin{bmatrix} w \\ \bar{w} \\ \check{w} \end{bmatrix} = \begin{bmatrix} E_c \\ \bar{E}_c \\ \check{E}_c \end{bmatrix} \begin{bmatrix} \tilde{y} \\ \tilde{x} \\ \tilde{x} \end{bmatrix},$$

where

$E_c \triangleq [E \ 0 \ 0]$ ,  $\bar{E}_c \triangleq [0 \ \bar{E} \ 0]$ ,  $\check{E}_c \triangleq [0 \ 0 \ \check{E}]$ , with (recall):  $E \triangleq \text{diag}([\hat{E}_i]_{i \in \mathbb{N}_N})$ ,  $\bar{E} \triangleq \text{diag}([\hat{\bar{E}}_l]_{l \in \mathbb{N}_L})$ , and  $\check{E} \triangleq \text{diag}([\hat{\check{E}}_m]_{m \in \mathbb{N}_M})$ , where

$$\hat{E}_i \triangleq \begin{bmatrix} 0 \\ 0 \\ \mathbf{I} \end{bmatrix}, \quad \hat{\bar{E}}_l \triangleq \begin{bmatrix} 0 \\ 0 \\ \mathbf{I} \end{bmatrix}, \quad \hat{\check{E}}_m \triangleq \begin{bmatrix} 0 \\ \mathbf{I} \end{bmatrix}.$$

### 5) Networked System Error Dynamics Representation:

Vectorizing the subsystem error dynamics in (61), (68), and (71) across all such subsystems along with their interconnection relationships including consolidated disturbance inputs and performance outputs yields the overall networked systems error dynamics representation.

For DG error subsystems, vectorizing (61), (62), and (66) across all  $i \in \mathbb{N}_N$  yields:

$$\begin{cases} \dot{\tilde{x}} = \tilde{A}\tilde{x} + \tilde{B}\tilde{\eta} + G(\tilde{x}), \\ \tilde{y} = C^y\tilde{x} + D^y\tilde{\eta}, \\ \tilde{\eta} = \tilde{K}\tilde{y} + \tilde{C}\tilde{x} + Ew, \end{cases} \quad (74)$$

where we define the error vectors:  $\tilde{x} \triangleq [\tilde{x}_i^\top]_{i \in \mathbb{N}_N}^\top$ ,  $\tilde{\eta} \triangleq [\tilde{\eta}_i^\top]_{i \in \mathbb{N}_N}^\top$ ,  $\tilde{y} \triangleq [\tilde{y}_i^\top]_{i \in \mathbb{N}_N}^\top$ ,  $\tilde{\tilde{x}} \triangleq [\tilde{\tilde{x}}_l^\top]_{l \in \mathbb{N}_L}^\top$ , the matrices:  $\tilde{A} \triangleq \text{diag}([\tilde{A}_i]_{i \in \mathbb{N}_N})$ ,  $C^y \triangleq \text{diag}([C_i^y]_{i \in \mathbb{N}_N})$ ,  $D^y \triangleq \text{diag}([D_i^y]_{i \in \mathbb{N}_N})$ , and the vector space:  $G(\tilde{x}) \triangleq [g_i^\top(\tilde{x}_i)]_{i \in \mathbb{N}_N}^\top$ .

For line error subsystems, vectorizing (68) and (69) across all  $l \in \mathbb{N}_L$  yields:

$$\begin{cases} \dot{\tilde{x}} = \bar{A}\tilde{x} + \hat{B}\tilde{\eta}, \\ \tilde{\eta} = C\tilde{y} + \check{C}\tilde{x} + \bar{E}\bar{w}, \end{cases} \quad (75)$$

where we define the error vectors:  $\tilde{\eta} \triangleq [\tilde{\eta}_l^\top]_{l \in \mathbb{N}_L}^\top$ , and  $\tilde{x} \triangleq [\tilde{x}_m^\top]_{m \in \mathbb{N}_M}^\top$ .

For load error subsystems, vectorizing (71) and (72) across all  $m \in \mathbb{N}_M$  yields:

$$\begin{cases} \dot{\tilde{x}} = \check{A}\tilde{x} + \hat{B}\tilde{\eta}, \\ \tilde{\eta} = \check{C}\tilde{x} + \check{E}\check{w}, \end{cases} \quad (76)$$

where we define the error vector:  $\tilde{\eta} \triangleq [\tilde{\eta}_m^\top]_{m \in \mathbb{N}_M}^\top$ .

The interconnection relationship among the error subsystems, as shown in Fig. 6, can now be identified as:

$$\begin{bmatrix} \tilde{\eta} \\ \tilde{\tilde{x}} \\ \tilde{\eta} \\ z_c \end{bmatrix} = \underbrace{\begin{bmatrix} \tilde{K} & \bar{C} & \mathbf{0} & E_c \\ C & \mathbf{0} & \check{C} & \bar{E}_c \\ \mathbf{0} & \check{C} & \mathbf{0} & \check{E}_c \\ H_c & \bar{H}_c & \check{H}_c & \mathbf{0} \end{bmatrix}}_{\triangleq \tilde{M}} \begin{bmatrix} \tilde{y} \\ \tilde{\tilde{x}} \\ \tilde{\tilde{x}} \\ w_c \end{bmatrix}^\top, \quad (77)$$

where  $\tilde{M}$  is the interconnection matrix.

## B. Equilibrium Point Analysis of the AC MG

The equilibrium point analysis enables the design of steady-state controllers that ensure the AC MG achieves simultaneous voltage regulation, frequency synchronization, and proportional power sharing objectives at steady state (equilibrium). We characterize the equilibrium point by constant states, where all time derivatives vanish, and are

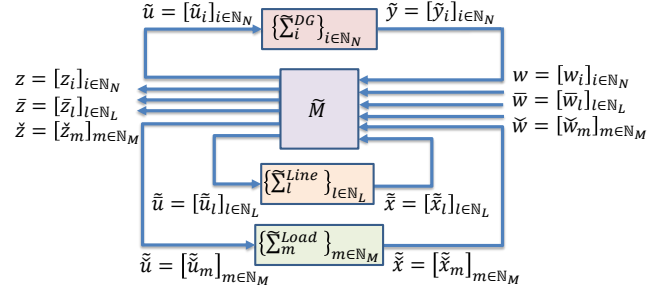


Fig. 6. Error networked system configuration showing interconnections between DGs, lines, and loads error dynamics in AC MG.

determined solely by steady-state inputs, reference signals, load parameters, and system parameters.

The incidence matrix  $\mathcal{B} \in \mathbb{R}^{(N+M) \times L}$  defined in (6) is partitioned as  $\mathcal{B} = [\mathcal{B}_D^\top \ \mathcal{B}_L^\top]^\top$ , where  $\mathcal{B}_D \in \mathbb{R}^{N \times L}$  corresponds to DG connections and  $\mathcal{B}_L \in \mathbb{R}^{M \times L}$  corresponds to load connections. The system parameter matrices are  $C_t \triangleq \text{diag}([C_{ti}]_{i \in \mathbb{N}_N})$ ,  $L_t \triangleq \text{diag}([L_{ti}]_{i \in \mathbb{N}_N})$ ,  $R_t \triangleq \text{diag}([R_{ti}]_{i \in \mathbb{N}_N})$ ,  $Y_L \triangleq \text{diag}([Y_{Li}]_{i \in \mathbb{N}_N})$ ,  $R \triangleq \text{diag}([R_l]_{l \in \mathbb{N}_L})$ ,  $L \triangleq \text{diag}([L_l]_{l \in \mathbb{N}_L})$ ,  $\check{C}_t \triangleq \text{diag}([C_{tm}]_{m \in \mathbb{N}_M})$ , and  $\check{Y}_L \triangleq \text{diag}([Y_{Lm}]_{m \in \mathbb{N}_M})$ . The complex impedance and admittance matrices are  $Z^{dq} \triangleq \text{diag}([R_l + i\omega_0 L_l]_{l \in \mathbb{N}_L})$ ,  $Z_t^{dq} \triangleq \text{diag}([R_{ti} + i\omega_0 L_{ti}]_{i \in \mathbb{N}_N})$ , and  $\check{Y}^{dq} \triangleq \text{diag}([Y_{Lm} + i\omega_0 C_{tm}]_{m \in \mathbb{N}_M})$ , with  $\Omega_0 \triangleq \text{diag}([i\omega_0]_{i \in \mathbb{N}_N})$ .

**Lemma 1:** Assuming all zero mean unknown disturbances components to be zero, i.e.,  $w_i(t) = 0, \forall i \in \mathbb{N}_N$ ,  $\bar{w}_l(t) = 0, \forall l \in \mathbb{N}_L$ ,  $\check{w}_m(t) = 0, \forall m \in \mathbb{N}_M$ , for a given reference voltage vector  $V_r \triangleq [V_{i,ref}^{dq}]_{i \in \mathbb{N}_N}$ , constant current load vectors  $\bar{I}_L \triangleq [\bar{I}_L^{dq}]_{i \in \mathbb{N}_N}$  and  $\check{I}_L \triangleq [\check{I}_L^{dq}]_{m \in \mathbb{N}_M}$ , under a fixed control input  $u_E^{Vdq} \triangleq [u_{Ei}^{Vdq}]_{i \in \mathbb{N}_N}$  defined as:

$$u_E^{Vdq} = V_r + Z_t^{dq}(Y_L V_r + \Omega_0 C_t V_r + \bar{I}_L + \mathcal{B}_D \bar{I}_E^{dq}), \quad (78)$$

there exists a unique equilibrium point for the AC MG characterized by reference voltage vector  $V_r$ , constant current load vectors  $\bar{I}_L$  and  $\check{I}_L$ , given by:

$$V_E^{dq} = V_r, \quad (79a)$$

$$\tilde{\omega}_E = \mathbf{0}, \quad (79b)$$

$$I_{tE}^{dq} = (Z_t^{dq})^{-1}(u_E^{dq} - V_E^{dq}), \quad (79c)$$

$$I_E^{dq} = (Z^{dq})^{-1}\mathcal{B}_D V_E^{dq} + (Z^{dq})^{-1}\mathcal{B}_L^\top \check{V}_E^{dq}, \quad (79d)$$

$$\check{V}_E^{dq} = -(\check{Y}^{dq})^{-1}(\check{I}_L^{dq} + \mathcal{B}_L I_E^{dq}), \quad (79e)$$

where we define the equilibrium state vectors  $V_E^{dq} \triangleq [V_{Ei}^{dq}]_{i \in \mathbb{N}_N} \in \mathbb{R}^{2N}$  (DG voltages),  $\tilde{\omega}_E \triangleq [\tilde{\omega}_{Ei}]_{i \in \mathbb{N}_N} \in \mathbb{R}^N$  (frequency deviations),  $I_{tE}^{dq} \triangleq [I_{tEi}^{dq}]_{i \in \mathbb{N}_N} \in \mathbb{R}^{2N}$  (DG filter currents),  $I_E^{dq} \triangleq [I_{Ei}^{dq}]_{i \in \mathbb{N}_N} \in \mathbb{R}^{2L}$  (line currents),  $\check{V}_E^{dq} \triangleq [V_{mE}^{dq}]_{m \in \mathbb{N}_M} \in \mathbb{R}^{2M}$  (load voltages).

**Proof:** At equilibrium, all state derivatives in the closed-loop system vanish. We establish the equilibrium conditions by analyzing each subsystem type.

**1) DG Subsystems:** The equilibrium state of the closed-loop DG dynamics of (60) satisfies:

$$\hat{A}_i x_{Ei} + \hat{B}_i \eta_{Ei} + \theta_i = 0,$$

where  $x_{Ei} \triangleq [V_{Ei}^d \ V_{Ei}^q \ I_{tEi}^d \ I_{tEi}^q \ v_{Ei}^d \ v_{Ei}^q \ \tilde{\omega}_{Ei}]^\top$  represents the equilibrium state,  $\eta_{Ei}$  represents the equilibrium effective input from (44), and using  $\hat{A}_i$  and  $\hat{B}_i$  defined in (40), we obtain from the respective rows:

$$-\frac{Y_{Li}}{C_{ti}}V_{Ei}^{dq} - i(\omega_0 + \tilde{\omega}_{Ei})V_{Ei}^{dq} + \frac{I_{tEi}^{dq}}{C_{ti}} - \frac{\bar{I}_{Li}^{dq}}{C_{ti}} - \frac{I_{Ei}^{dq}}{C_{ti}} = 0, \quad (80)$$

$$-\frac{V_{Ei}^{dq}}{L_{ti}} - \left( \frac{R_{ti}}{L_{ti}} + i(\omega_0 + \tilde{\omega}_{Ei}) \right) I_{tEi}^{dq} + \frac{u_{Ei}^{Vdq}}{L_{ti}} = 0, \quad (81)$$

$$V_{Ei}^{dq} - V_{i,ref}^{dq} = 0, \quad (82)$$

$$-\frac{1}{\tau_i} \tilde{\omega}_{Ei} + \frac{1}{\tau_i} u_{Ei}^\Omega = 0. \quad (83)$$

From (82), we directly obtain:

$$V_{Ei}^{dq} = V_{i,ref}^{dq}, \quad (84)$$

which vectorizes to establish (79a). From (83), we have  $\tilde{\omega}_{Ei} = u_{Ei}^\Omega$ , where under the normalized power sharing control law (25):

$$u_{Ei}^\Omega = \sum_{j \in \mathcal{N}_i^C} K_{ij}^\Omega (P_{n,Ei} - P_{n,Ej}),$$

with  $P_{n,Ei} = P_{Ei}/P_i^{\max}$  representing the normalized active power of  $\Sigma_i^{DG}$ . At equilibrium  $P_{n,Ei} = P_{n,Ej}$  for all  $j \in \mathcal{N}_i^C$ , which implies that each term in the summation vanishes. Therefore,  $u_{Ei}^\Omega = 0$  and thus  $\tilde{\omega}_{Ei} = 0$  for all  $i \in \mathbb{N}_N$ , establishing (79b).

With  $\tilde{\omega}_{Ei} = 0$ , (81) simplifies to:

$$-\frac{V_{Ei}^{dq}}{L_{ti}} - \left( \frac{R_{ti}}{L_{ti}} + i\omega_0 \right) I_{tEi}^{dq} + \frac{u_{Ei}^{Vdq}}{L_{ti}} = 0,$$

which by multiplying by  $L_{ti}$  and rearranging yields:

$$u_{Ei}^{Vdq} = V_{Ei}^{dq} + (R_{ti} + i\omega_0 L_{ti}) I_{tEi}^{dq},$$

where defining the  $i$ -th diagonal element of  $Z_t$  as  $Z_{t,i}^{dq} \triangleq R_{ti} + i\omega_0 L_{ti}$ , gives:

$$u_{Ei}^{Vdq} = V_{Ei}^{dq} + Z_{t,i}^{dq} I_{tEi}^{dq}. \quad (85)$$

Solving for the equilibrium filter current and substituting  $V_{Ei}^{dq} = V_{i,ref}^{dq}$  from (84):

$$I_{tEi}^{dq} = (Z_{t,i}^{dq})^{-1} (u_{Ei}^{Vdq} - V_{i,ref}^{dq}),$$

which vectorizes for  $i \in \mathbb{N}_N$  yield:

$$I_{tE}^{dq} = (Z_t^{dq})^{-1} (u_E^{Vdq} - V_r), \quad (86)$$

establishing (79c).

With  $\tilde{\omega}_{Ei} = 0$ , (80) can be written by multiplying by  $C_{ti}$  and substituting  $I_{Ei}^{dq} = \sum_{l \in \mathcal{E}_i} \mathcal{B}_{il} I_{El}^{dq}$ :

$$-Y_{Li} V_{Ei}^{dq} - i\omega_0 C_{ti} V_{Ei}^{dq} + I_{tEi}^{dq} - \bar{I}_{Li}^{dq} - \sum_{l \in \mathcal{E}_i} \mathcal{B}_{il} I_{El}^{dq} = 0,$$

which rearranges to gives:

$$I_{tEi}^{dq} = (Y_{Li} + i\omega_0 C_{ti}) V_{Ei}^{dq} + \bar{I}_{Li}^{dq} + \sum_{l \in \mathcal{E}_i} \mathcal{B}_{il} I_{El}^{dq}.$$

Substituting the expression for  $I_{tEi}^{dq}$  from (86) and  $V_{Ei}^{dq} = V_{i,ref}^{dq}$  from (84) yields:

$$(Z_{t,i}^{dq})^{-1} (u_{Ei}^{Vdq} - V_{i,ref}^{dq}) = (Y_{Li} + i\omega_0 C_{ti}) V_{i,ref}^{dq} + \bar{I}_{Li}^{dq} + \sum_{l \in \mathcal{E}_i} \mathcal{B}_{il} I_{El}^{dq}$$

which by multiplying both sides by  $Z_{t,i}^{dq}$  and rearranging

gives:

$$u_{Ei}^{Vdq} = V_{i,ref}^{dq} + Z_{t,i}^{dq} \left( (Y_{Li} + i\omega_0 C_{ti}) V_{i,ref}^{dq} + \bar{I}_{Li}^{dq} + \sum_{l \in \mathcal{E}_i} \mathcal{B}_{il} I_{El}^{dq} \right).$$

Note that  $\sum_{l \in \mathcal{E}_i} \mathcal{B}_{il} I_{El}^{dq} = [\mathcal{B}_D I_{El}^{dq}]_i$  is the  $i$ -th component of the vector  $\mathcal{B}_D I_{El}^{dq}$ . Vectorizing for all  $i \in \mathbb{N}_N$  with  $\Omega_0 \triangleq \text{diag}([i\omega_0]_{i \in \mathbb{N}_N})$ :

$$u_E^{Vdq} = V_r + Z_t^{dq} \left( (Y_L + \Omega_0 C_t) V_r + \bar{I}_L + \mathcal{B}_D I_E^{dq} \right),$$

which can be rewritten as:

$$u_E^{Vdq} = V_r + Z_t^{dq} (Y_L V_r + \Omega_0 C_t V_r + \bar{I}_L + \mathcal{B}_D I_E^{dq}),$$

establishing (78).

2) **Line Subsystems:** The equilibrium state of the line dynamics from (67) satisfies:

$$\bar{A}_l \bar{x}_{El} + \hat{B}_l \bar{\eta}_{lE} = 0,$$

where  $\bar{x}_{El} = I_{El}^{dq}$  and  $\bar{\eta}_{lE}$  is the equilibrium effective input of (69) given by:

$$\bar{\eta}_{lE} = \begin{bmatrix} \sum_{k \in \mathcal{N}_l^P \cap \mathcal{D}} C_{lk} y_{Ek} \\ \sum_{m \in \mathcal{N}_l^P \cap \mathcal{L}} \check{C}_{lm} \check{x}_{Em} \\ \mathbf{0} \end{bmatrix}.$$

From (48) and (49), we can extract voltages as  $\sum_{k \in \mathcal{N}_l^P} C_{lk} y_{Ek} = \sum_{k \in \mathcal{N}_l^P} \mathcal{B}_{kl} V_{Ek}^{dq}$ ,  $\sum_{m \in \mathcal{N}_l^P} \check{C}_{lm} \check{x}_{Em} = \sum_{m \in \mathcal{N}_l^P} \mathcal{B}_{ml} V_{mE}^{dq}$ , respectively. Using  $\bar{A}_l$  and  $\bar{B}_l$  from (19) gives:

$$-\left( \frac{R_l}{L_l} + i\omega_0 \right) I_{El}^{dq} + \frac{1}{L_l} \sum_{k \in \mathcal{N}_l^P} \mathcal{B}_{kl} V_{Ek}^{dq} = 0,$$

which by multiplying by  $L_l$  and rearranging:

$$(R_l + i\omega_0 L_l) I_{El}^{dq} = \sum_{k \in \mathcal{N}_l^P} \mathcal{B}_{kl} V_{Ek}^{dq},$$

where defining the  $l$ -th diagonal element of  $Z^{dq}$  as  $Z_l^{dq} \triangleq R_l + i\omega_0 L_l$  gives:

$$I_{El}^{dq} = (Z_l^{dq})^{-1} \sum_{k \in \mathcal{N}_l^P} \mathcal{B}_{kl} V_{Ek}^{dq}.$$

This summation can be decomposed as

$$\sum_{k \in \mathcal{N}_l^P} \mathcal{B}_{kl} V_{Ek}^{dq} = \sum_{i \in \mathcal{N}_l^P \cap \mathcal{D}} \mathcal{B}_{il} V_{Ei}^{dq} + \sum_{m \in \mathcal{N}_l^P \cap \mathcal{L}} \mathcal{B}_{ml} V_{mE}^{dq} = [\mathcal{B}_D^\top V_E^{dq}]_l + [\mathcal{B}_L^\top V_{mE}^{dq}]_l,$$

where the first term corresponds to DG contributions and the second to load contributions. Therefore:

$$I_{El}^{dq} = (Z_l^{dq})^{-1} ([\mathcal{B}_D^\top V_E^{dq}]_l + [\mathcal{B}_L^\top V_{mE}^{dq}]_l),$$

which vectorizes for all  $l \in \mathbb{N}_L$  yields:

$$I_{El}^{dq} = (Z^{dq})^{-1} \mathcal{B}_D^\top V_E^{dq} + (Z^{dq})^{-1} \mathcal{B}_L^\top V_{mE}^{dq},$$

establishing (79d).

3) **Load Subsystems:** The equilibrium state of the load dynamics from (70) satisfies:

$$\check{A}_m \check{x}_{Em} + \hat{B}_m \check{\eta}_{mE} + \check{\theta}_m = 0,$$

where  $\check{x}_{Em} = V_{mE}^{dq}$  and  $\check{\eta}_{mE}$  is the equilibrium effective input of (72) given by:

$$\check{\eta}_{mE} = \begin{bmatrix} \sum_{l \in \mathcal{E}_m} \check{C}_{ml} \check{x}_{El} \\ \mathbf{0} \end{bmatrix}.$$

From (53), we obtain  $\sum_{l \in \mathcal{E}_m} \bar{C}_{ml} \bar{x}_{El} = \sum_{l \in \mathcal{E}_m} \mathcal{B}_{ml} I_{El}^{dq}$ , which using  $\check{A}_m$  and  $\hat{B}_m$  from (15) gives:

$$-\left(\frac{Y_{Lm}}{C_{tm}} + i\omega_0\right) V_{mE}^{dq} - \frac{1}{C_{tm}} \left( \sum_{l \in \mathcal{E}_m} \mathcal{B}_{ml} I_{El}^{dq} + \bar{I}_{Lm}^{dq} \right) = 0.$$

Multiplying by  $C_{tm}$  and rearranging yields:

$$-(Y_{Lm} + i\omega_0 C_{tm}) V_{mE}^{dq} = \sum_{l \in \mathcal{E}_m} \mathcal{B}_{ml} I_{El}^{dq} + \bar{I}_{Lm}^{dq},$$

where defining the  $m$ -th diagonal element of  $Y^{dq}$  as  $Y_m^{dq} \triangleq Y_{Lm} + i\omega_0 C_{tm}$  gives:

$$V_{mE}^{dq} = -(Y_m^{dq})^{-1} \left( \bar{I}_{Lm}^{dq} + \sum_{l \in \mathcal{E}_m} \mathcal{B}_{ml} I_{El}^{dq} \right).$$

Note that  $\sum_{l \in \mathcal{E}_m} \mathcal{B}_{ml} I_{El}^{dq} = [\mathcal{B}_{Ll} I_{El}^{dq}]_m$  is the  $m$ -th component of  $\mathcal{B}_{Ll} I_{El}^{dq}$ . Vectorizing for all  $m \in \mathbb{N}_M$  yields:

$$V_{mE}^{dq} = -(Y^{dq})^{-1} \left( \bar{I}_{Lm}^{dq} + \mathcal{B}_{Ll} I_E^{dq} \right),$$

establishing (79e).

This completes the proof. The coupled equations (78) and (79) uniquely determine all equilibrium state variables.  $\blacksquare$

**Remark 4:** At equilibrium, we require the condition for proportional power sharing among DGs to be met, and thus we require

$$\begin{aligned} \frac{P_{Ei}}{P_{\max}} &= P_s \iff P_{Ei} = P_i^{\max} P_s, \quad \forall i \in \mathbb{N}_N, \\ \frac{Q_{Ei}}{Q_i^{\max}} &= Q_s \iff Q_{Ei} = Q_i^{\max} Q_s, \quad \forall i \in \mathbb{N}_N, \end{aligned} \quad (87)$$

which can be expressed in vectorized form as  $P_E = P_{\max} \mathbf{1}_N P_s$  and  $Q_E = Q_{\max} \mathbf{1}_N Q_s$ , where  $P_{\max} \triangleq \text{diag}([P_i^{\max}]_{i \in \mathbb{N}_N})$  and  $Q_{\max} \triangleq \text{diag}([Q_i^{\max}]_{i \in \mathbb{N}_N})$ . Using this requirement, the distributed control components at equilibrium become zero:

$$u_{iG,E}^{dq} = \begin{bmatrix} u_{iE}^P \\ u_{iE}^Q \\ u_{iE}^{\Omega} \end{bmatrix} = \mathbf{0}, \quad \forall i \in \mathbb{N}_N,$$

since proportional power sharing is achieved. From (85), we have

$$u_{Ei}^{Vdq} = V_{i,\text{ref}}^{dq} + Z_{t,i}^{dq} I_{tEi}^{dq}, \quad \forall i \in \mathbb{N}_N.$$

Therefore, to achieve this particular control equilibrium (which satisfies voltage regulation, frequency synchronization, and proportional power sharing objectives), we need to select our steady-state control input in (29) as:

$$u_{iS}^{dq} = V_{i,\text{ref}}^{dq} + Z_{t,i}^{dq} I_{tEi}^{dq}, \quad \forall i \in \mathbb{N}_N, \quad (88)$$

where  $Z_{t,i}^{dq} \triangleq R_{ti} + i\omega_0 L_{ti}$  and  $I_{tEi}^{dq}$  is determined by the network equilibrium equations (79c) under the power sharing constraint (87). This is because at the equilibrium point, local control  $u_{iL}^{dq}$  (21) and distributed global control  $u_{iG}^{dq}$  (28) components are, by definition, zero for any  $i \in \mathbb{N}_N$ .

In conclusion, using Lemma 1 and Remark 4, for the equilibrium of AC MG to satisfy the voltage regulation, frequency synchronization, and proportional power sharing

conditions, we require:

$$\begin{aligned} u_E^{Vdq} &= V_r + Z_t^{dq} (Y_L V_r + \Omega_0 C_t V_r + \bar{I}_L + \mathcal{B}_D I_E^{dq}) \\ &= V_r + Z_t^{dq} I_{tE}^{dq} = u_S^{dq}, \\ V_E^{dq} &= V_r, \\ \tilde{\omega}_E &= \mathbf{0}, \\ P_E &= P_{\max} \mathbf{1}_N P_s, \quad Q_E = Q_{\max} \mathbf{1}_N Q_s, \\ I_{tE}^{dq} &= (Z^{dq})^{-1} (u_E^{Vdq} - V_E^{dq}), \\ I_E^{dq} &= (Z^{dq})^{-1} \mathcal{B}_D^\top V_E^{dq} + (Z^{dq})^{-1} \mathcal{B}_L^\top V_{mE}^{dq}, \\ V_{mE}^{dq} &= -(Y^{dq})^{-1} (\bar{I}_{Lm}^{dq} + \mathcal{B}_L I_E^{dq}). \end{aligned} \quad (89)$$

**Theorem 1:** To ensure the existence of an equilibrium point that satisfies the voltage regulation, frequency synchronization, and power sharing objectives, the reference voltages  $V_{i,\text{ref}}$  and power sharing coefficients  $P_s$  and  $Q_s$  should be a feasible solution in the optimization problem:

$$\min_{V_r, P_s, Q_s} \alpha_V \|V_r - \bar{V}_r\|^2 + \alpha_P P_s + \alpha_Q Q_s$$

Sub. to:  $V_{\min} \leq |V_r| \leq V_{\max}$ ,  $0 \leq P_s \leq 1$ ,  $0 \leq Q_s \leq 1$ ,

$$P_{\max} \mathbf{1}_N P_s = \text{diag}(V_r^d) I_E^d + \text{diag}(V_r^q) I_E^q,$$

$$Q_{\max} \mathbf{1}_N Q_s = \text{diag}(V_r^q) I_E^d - \text{diag}(V_r^d) I_E^q, \quad (90)$$

where  $V_r = [V_{i,\text{ref}}^{dq}]_{i \in \mathbb{N}_N}$ ,  $V_r^d$  and  $V_r^q$  are the  $d$  and  $q$  components of  $V_r$ ,  $I_E^{dq}$  is determined from the network equilibrium equations (79d)-(79e) as a function of  $V_r$ ,  $P_{\max} \triangleq \text{diag}([P_i^{\max}]_{i \in \mathbb{N}_N})$ ,  $Q_{\max} \triangleq \text{diag}([Q_i^{\max}]_{i \in \mathbb{N}_N})$ ,  $\bar{V}_r$  are desired reference voltage values, and  $\alpha_V > 0$ ,  $\alpha_P > 0$ , and  $\alpha_Q > 0$  are normalizing cost coefficients.

Overall, this formulation ensures proper system operation through multiple aspects. The equality constraints guarantee that both active and reactive proportional power sharing objectives are achieved across all DGs simultaneously. The reference voltage magnitude bounds maintain system operation within safe and efficient limits. Furthermore, the constraints on  $P_s$  and  $Q_s$  ensure that the power sharing coefficients remain properly normalized for practical implementations.

The AC MG requires two sets of coupled equality constraints, one for active power and one for reactive power, due to the dual power flow objectives inherent to AC systems. These equality constraints couple the power sharing requirements with the network power flow equations (9), where the line injection currents  $I_E^{dq}$  depend on the reference voltages through the network equilibrium relationships (79d)-(79e). This introduces additional complexity in determining a feasible set of reference voltages and power sharing coefficients that simultaneously satisfy voltage regulation, frequency synchronization, and proportional power sharing objectives.

## VI. DISSIPATIVITY-BASED CONTROL AND TOPOLOGY CO-DESIGN

This section analyzes the dissipativity properties of the AC MG error subsystems and formulates the global control and topology co-design problem. We establish necessary conditions for subsystem passivity indices and synthesize local controllers to ensure global feasibility.

Consider the DG error subsystem  $\tilde{\Sigma}_i^{DG}, i \in \mathbb{N}_N$  from (61). We characterize this subsystem as  $X_i$ -EID with supply rate matrix

$$X_i = \begin{bmatrix} X_i^{11} & X_i^{12} \\ X_i^{21} & X_i^{22} \end{bmatrix} \triangleq \begin{bmatrix} -\nu_i \mathbf{I} & \frac{1}{2} \mathbf{I} \\ \frac{1}{2} \mathbf{I} & -\rho_i \mathbf{I} \end{bmatrix}, \quad (91)$$

where  $\rho_i > 0$  and  $\nu_i < 0$  are the output and input passivity indices of  $\tilde{\Sigma}_i^{DG}$ , respectively. Thus,  $\tilde{\Sigma}_i^{DG}, i \in \mathbb{N}_N$  is strictly passive with IF-OFP( $\nu_i, \rho_i$ ).

Similarly, for the line subsystem  $\tilde{\Sigma}_l^{Line}, l \in \mathbb{N}_L$  described by (68), we assume it is  $\tilde{X}_l$ -EID with supply rate matrix

$$\tilde{X}_l = \begin{bmatrix} \tilde{X}_l^{11} & \tilde{X}_l^{12} \\ \tilde{X}_l^{21} & \tilde{X}_l^{22} \end{bmatrix} \triangleq \begin{bmatrix} -\bar{\nu}_l \mathbf{I} & \frac{1}{2} \mathbf{I} \\ \frac{1}{2} \mathbf{I} & -\bar{\rho}_l \mathbf{I} \end{bmatrix}, \quad (92)$$

where  $\bar{\rho}_l > 0$  and  $\bar{\nu}_l < 0$  are output and input passivity indices of the line subsystem, making  $\tilde{\Sigma}_l^{Line}$  strictly passive with IF-OFP( $\bar{\nu}_l, \bar{\rho}_l$ ).

Additionally, for the load error subsystem  $\tilde{\Sigma}_m^{Load}, m \in \mathbb{N}_M$  from (71), we assume it is  $\tilde{X}_m$ -EID with supply rate matrix

$$\tilde{X}_m = \begin{bmatrix} \tilde{X}_m^{11} & \tilde{X}_m^{12} \\ \tilde{X}_m^{21} & \tilde{X}_m^{22} \end{bmatrix} \triangleq \begin{bmatrix} -\check{\nu}_m \mathbf{I} & \frac{1}{2} \mathbf{I} \\ \frac{1}{2} \mathbf{I} & -\check{\rho}_m \mathbf{I} \end{bmatrix}, \quad (93)$$

where  $\check{\rho}_m > 0$  and  $\check{\nu}_m < 0$  are the output and input passivity indices of the load subsystem, making  $\tilde{\Sigma}_m^{Load}$  strictly passive with IF-OFP( $\check{\nu}_m, \check{\rho}_m$ ).

**Lemma 2:** For the frequency coupling nonlinearity  $g_i(\tilde{x}_i)$  defined in (63), there exists a scalar  $\beta_i \triangleq \sqrt{C_{ti}^2 \bar{V}_{tot}^2 + L_{ti}^2 \bar{I}_{tot}^2}$  (where  $\bar{V}_{tot} = \bar{V} + \|V_{Ei}^{dq}\|$  and  $\bar{I}_{tot} = \bar{I} + \|I_{tEi}^{dq}\|$  with  $\bar{V}, \bar{I} > 0$ ) such that for all  $\tilde{x}_i$  in the operating region satisfying  $\|\tilde{V}_i^{dq}\| \leq \bar{V}$  and  $\|\tilde{I}_{ti}^{dq}\| \leq \bar{I}$ , the norm bound

$$\|g_i(\tilde{x}_i)\|^2 \leq \tilde{\omega}_i^2 \cdot \beta_i^2, \quad (94)$$

holds, which is equivalent to the quadratic constraint

$$\begin{bmatrix} \tilde{x}_i \\ g_i(\tilde{x}_i) \end{bmatrix}^\top \Psi_i \begin{bmatrix} \tilde{x}_i \\ g_i(\tilde{x}_i) \end{bmatrix} \geq 0, \quad (95)$$

where:

$$\Psi_i = \begin{bmatrix} \beta_i^2 e_7 e_7^\top & \mathbf{0}_{7 \times 7} \\ \mathbf{0}_{7 \times 7} & -\mathbf{I}_7 \end{bmatrix} \in \mathbb{R}^{14 \times 14}, \quad (96)$$

and  $e_7$  is the unit vector in  $\mathbb{R}^{7 \times 1}$  with a 1 in the last element.

*Proof:* The frequency coupling nonlinearity  $g_i(\tilde{x}_i)$  has the structure given in (63), which yields:

$$\|g_i(\tilde{x}_i)\|^2 = \tilde{\omega}_i^2 \left( \|V_i^{dq}\|^2 + \|I_{ti}^{dq}\|^2 \right).$$

From the error variable definitions (58a) and (58b), we have  $V_i^{dq} = \tilde{V}_i^{dq} + V_{Ei}^{dq}$  and  $I_{ti}^{dq} = \tilde{I}_{ti}^{dq} + I_{tEi}^{dq}$ . Applying the triangle inequality in the operating region where  $\|\tilde{V}_i^{dq}\| \leq \bar{V}$  and  $\|\tilde{I}_{ti}^{dq}\| \leq \bar{I}$ , we obtain:

$$\begin{aligned} \|V_i^{dq}\| &\leq \|\tilde{V}_i^{dq}\| + \|V_{Ei}^{dq}\| \leq \bar{V} + \|V_{Ei}^{dq}\| \triangleq \bar{V}_{tot}, \\ \|I_{ti}^{dq}\| &\leq \|\tilde{I}_{ti}^{dq}\| + \|I_{tEi}^{dq}\| \leq \bar{I} + \|I_{tEi}^{dq}\| \triangleq \bar{I}_{tot}. \end{aligned}$$

Weighting the voltage and current contributions by the physical system parameters  $C_{ti}$  and  $L_{ti}$  to account for their relative magnitudes in the energy storage, we establish:

$$\|g_i(\tilde{x}_i)\|^2 \leq \tilde{\omega}_i^2 \left( C_{ti}^2 \bar{V}_{tot}^2 + L_{ti}^2 \bar{I}_{tot}^2 \right) = \tilde{\omega}_i^2 \cdot \beta_i^2,$$

which is equation (94). Rearranging (94) gives  $\beta_i^2 \tilde{\omega}_i^2 - \|g_i(\tilde{x}_i)\|^2 \geq 0$ . Since  $\tilde{\omega}_i = e_7^\top \tilde{x}_i$ , expanding the quadratic

form yields:

$$\begin{aligned} \begin{bmatrix} \tilde{x}_i \\ g_i(\tilde{x}_i) \end{bmatrix}^\top \Psi_i \begin{bmatrix} \tilde{x}_i \\ g_i(\tilde{x}_i) \end{bmatrix} &= \tilde{x}_i^\top (\beta_i^2 e_7 e_7^\top) \tilde{x}_i + g_i(\tilde{x}_i)^\top (-\mathbf{I}_7) g_i(\tilde{x}_i), \\ &= \beta_i^2 (e_7^\top \tilde{x}_i)^2 - \|g_i(\tilde{x}_i)\|^2 = \beta_i^2 \tilde{\omega}_i^2 - \|g_i(\tilde{x}_i)\|^2, \end{aligned}$$

establishing the equivalence between (94) and (95) and completing the proof.  $\blacksquare$

**Theorem 2:** Under the quadratic constraint on the frequency coupling nonlinearity established in Lemma 2, the DG error subsystem  $\tilde{\Sigma}_i^{DG} : \tilde{\eta}_i \rightarrow \tilde{y}_i, i \in \mathbb{N}_N$  described by (61) with linearized output (66) can be made IF-OFP( $\nu_i, \rho_i$ ) (as assumed in (91)) by designing the local controller gain matrix  $K_{i0}$  from (21) that solves the LMI feasibility problem:

Find:  $\tilde{K}_{i0}, \tilde{P}_i, \tilde{R}_i, \tilde{\lambda}_i, \nu_i$ , and  $\tilde{\rho}_i$ ,

s.t.:  $\tilde{P}_i > 0, \tilde{R}_i > 0, \tilde{\lambda}_i > 0, \nu_i < 0$ , and  $\tilde{\rho}_i > 0$ ,

$$\begin{bmatrix} \Phi_i & \tilde{R}_i & \mathbf{0} & \mathbf{0} \\ \tilde{R}_i & \tilde{R}_i & \tilde{P}_i & \mathbf{0} \\ \mathbf{0} & \tilde{P}_i & -\mathcal{H}(A_i \tilde{P}_i + B_i \tilde{K}_{i0}) + \tilde{\lambda}_i \mathbf{I} & -\mathbf{I} + \frac{1}{2} \tilde{P}_i \\ \mathbf{0} & \mathbf{0} & -\mathbf{I} + \frac{1}{2} \tilde{P}_i & -\nu_i \mathbf{I} \end{bmatrix} > 0, \quad (97)$$

where  $\Phi_i \triangleq \tilde{\rho}_i \mathbf{I} + \tilde{R}_i - \tilde{\lambda}_i \beta_i^2 e_7 e_7^\top, K_{i0} \triangleq \tilde{K}_{i0} \tilde{P}_i^{-1}, \rho_i \triangleq \tilde{\rho}_i^{-1}$ ,  $e_7$  is the unit vector in  $\mathbb{R}^{7 \times 1}$  with a 1 in the last element, and  $\beta_i$  are defined in Lemma 2.

*Proof:* We establish that the DG error subsystem  $\tilde{\Sigma}_i^{DG}, i \in \mathbb{N}_N$  from (61) can be made IF-OFP( $\nu_i, \rho_i$ ) by synthesizing the local controller gain  $K_{i0}$  through solving an LMI problem. Consider a quadratic storage function  $V_i(\tilde{x}_i) = \tilde{x}_i^\top P_i \tilde{x}_i$  with  $P_i > 0$ . The time derivative  $\dot{V}_i = 2\tilde{x}_i^\top P_i \dot{\tilde{x}}_i$  can be written in symmetric form as:

$$\dot{V}_i = \begin{bmatrix} \dot{\tilde{x}}_i \\ \tilde{x}_i \end{bmatrix}^\top \begin{bmatrix} P_i & \mathbf{0} \\ \mathbf{0} & P_i \end{bmatrix} \begin{bmatrix} \dot{\tilde{x}}_i \\ \tilde{x}_i \end{bmatrix}.$$

To handle the nonlinearity  $g_i(\tilde{x}_i)$  from (63) systematically, we introduce an augmented vector  $\zeta_i \triangleq [\tilde{\eta}_i^\top \ \tilde{x}_i^\top \ g_i^\top]^\top$  and define the structured matrix:

$$\Theta_i \triangleq \begin{bmatrix} \hat{B}_i & \hat{A}_i & \mathbf{I} \\ \mathbf{0} & \mathbf{I} & \mathbf{0} \end{bmatrix},$$

where  $\hat{A}_i = A_i + B_i K_{i0}$  and  $\hat{B}_i = [B_i \ F_i \ E_i]^\top$  from (40). This structured representation yields  $[\dot{\tilde{x}}_i \ \tilde{x}_i]^\top = \Theta_i \zeta_i$ , and substituting into the storage function derivatives gives:

$$\dot{V}_i = \zeta_i^\top \Theta_i^\top \begin{bmatrix} P_i & \mathbf{0} \\ \mathbf{0} & P_i \end{bmatrix} \Theta_i \zeta_i.$$

For the IF-OFP( $\nu_i, \rho_i$ ) property with supply rate matrix from (91), we require the dissipation inequality:

$$\dot{V}_i \leq \begin{bmatrix} \tilde{\eta}_i \\ \tilde{y}_i \end{bmatrix}^\top X_i \begin{bmatrix} \tilde{\eta}_i \\ \tilde{y}_i \end{bmatrix}. \quad (98)$$

From (66), the linearized output satisfies  $\tilde{y}_i = C_i^y \tilde{x}_i + D_i^y \tilde{\eta}_i$ . We define the output mapping matrix:

$$\bar{\Theta}_i \triangleq \begin{bmatrix} \mathbf{I} & \mathbf{0} & \mathbf{0} \\ D_i^y & C_i^y & \mathbf{0} \end{bmatrix},$$

such that  $[\tilde{\eta}_i \ \tilde{y}_i]^\top = \bar{\Theta}_i \zeta_i$ . Combining these expressions with (98), the dissipativity condition becomes:

$$\zeta_i^\top (\Theta_i^\top \Pi_i \Theta_i - \bar{\Theta}_i^\top X_i \bar{\Theta}_i) \zeta_i \leq 0,$$

where  $\Pi_i \triangleq \text{diag}(P_i, P_i)$ . Defining  $W_i \triangleq \Theta_i^\top \Pi_i \Theta_i - \bar{\Theta}_i^\top X_i \bar{\Theta}_i$ , we require  $W_i \leq 0$ , but this condition must only hold for trajectories satisfying the frequency coupling constraint from Lemma 2.

From (95) in Lemma 2, the nonlinearity satisfies the quadratic constraint:

$$\begin{bmatrix} \tilde{x}_i \\ g_i(\tilde{x}_i) \end{bmatrix}^\top \Psi_i \begin{bmatrix} \tilde{x}_i \\ g_i(\tilde{x}_i) \end{bmatrix} \geq 0,$$

where  $\Psi_i$  is defined in (96). Embedding this constraint into the augmented space, we define:

$$\bar{\Psi}_i \triangleq \begin{bmatrix} \mathbf{0} & \mathbf{0} & \mathbf{0} \\ \mathbf{0} & \beta_i^2 e_7 e_7^\top & \mathbf{0} \\ \mathbf{0} & \mathbf{0} & -\mathbf{I} \end{bmatrix},$$

where  $e_7$  is the unit vector in  $\mathbb{R}^{7 \times 1}$  with a 1 in the last element. The constraint then becomes  $\zeta_i^\top \bar{\Psi}_i \zeta_i \geq 0$ . By the S-procedure, if there exists  $\lambda_i > 0$  such that:

$$W_i - \lambda_i \bar{\Psi}_i \leq 0,$$

then  $\zeta_i^\top W_i \zeta_i \leq 0$  holds for all  $\zeta_i$  satisfying the nonlinearity constraint. Expanding this condition yields:

$$\Theta_i^\top \Pi_i \Theta_i - \bar{\Theta}_i^\top X_i \bar{\Theta}_i - \lambda_i \bar{\Psi}_i \leq 0.$$

To obtain an LMI formulation suitable for controller synthesis, we apply Proposition 1 with variable transformations  $\tilde{P}_i = P_i^{-1}$  and  $\tilde{K}_{i0} = K_{i0} \tilde{P}_i$ . Additionally, we define  $\tilde{\lambda}_i = \lambda_i^{-1}$  and  $\tilde{\rho}_i = \rho_i^{-1}$  to convert the inequality constraints into a convex LMI form. Introducing an auxiliary slack variable  $\tilde{R}_i = R_i^{-1} > 0$  from the S-procedure transformation and applying congruence transformations with  $\text{diag}(\tilde{R}_i, \tilde{R}_i, \tilde{P}_i, \mathbf{I})$  followed by Schur complements, we obtain the LMI (97), where  $K_{i0} \triangleq \tilde{K}_{i0} \tilde{P}_i^{-1}$  and  $\rho_i \triangleq \tilde{\rho}_i^{-1}$ . The notation  $\Phi_i \triangleq \tilde{\rho}_i \mathbf{I} + \tilde{R}_i - \tilde{\lambda}_i \beta_i^2 e_7 e_7^\top$  compactly represents the first block of the LMI, which encodes both the passivity constraint and the frequency coupling bound. This completes the proof. ■

**Lemma 3:** For  $\tilde{\Sigma}_l^{Line}, l \in \mathbb{N}_L$  (68), the passivity indices  $\bar{\nu}_l$ , and  $\bar{\rho}_l$  from (92) can be characterized by solving the LMI problem:

Find:  $\bar{P}_l, \bar{\nu}_l$ , and  $\bar{\rho}_l$ ,

$$\text{s.t.: } \bar{P}_l > 0, \begin{bmatrix} -\mathcal{H}(\bar{P}_l \bar{A}_l) - \bar{\rho}_l \mathbf{I}_2 & -\bar{P}_l \bar{B}_l + \frac{1}{2} \mathbf{I}_2 \\ * & -\bar{\nu}_l \mathbf{I}_2 \end{bmatrix} \geq \mathbf{0}, \quad (99)$$

with maximum feasible passivity indices  $\bar{\nu}_l^{\max} = 0$  and  $\bar{\rho}_l^{\max} = R_l \mathbf{I}_2$  achieved when  $\bar{P}_l = \frac{L_l}{2} \mathbf{I}_2$ .

*Proof:* For  $\tilde{\Sigma}_l^{Line}, l \in \mathbb{N}_L$  described by (68), we establish its  $\bar{X}_l$ -dissipativity with the passivity indices in (92). We consider the output as  $\tilde{y}_l = \tilde{x}_l$  (i.e.,  $\bar{C}_l = \mathbf{I}_2$  and  $\bar{D}_l = \mathbf{0}$ ). Applying Prop. 1 with the system matrices from (19) and the dissipativity supply rate form in (92), we obtain:

$$\begin{bmatrix} -\mathcal{H}(\bar{P}_l \bar{A}_l) + \bar{C}_l^\top \bar{X}_l^{22} \bar{C}_l & -\bar{P}_l \bar{B}_l + \bar{C}_l^\top \bar{X}_l^{21} + \bar{C}_l^\top \bar{X}_l^{22} \bar{D}_l \\ * & \bar{X}_l^{11} + \mathcal{H}(\bar{X}_l^{12} \bar{D}_l) + \bar{D}_l^\top \bar{X}_l^{22} \bar{D}_l \end{bmatrix} \geq \mathbf{0}.$$

Substituting  $\bar{C}_l = \mathbf{I}_2$ ,  $\bar{D}_l = \mathbf{0}$ , and the components of  $\bar{X}_l$  from (92), we obtain:

$$\begin{bmatrix} -\mathcal{H}(\bar{P}_l \bar{A}_l) - \bar{\rho}_l \mathbf{I}_2 & -\bar{P}_l \bar{B}_l + \frac{1}{2} \mathbf{I}_2 \\ * & -\bar{\nu}_l \mathbf{I}_2 \end{bmatrix} \geq \mathbf{0},$$

which is the LMI condition in (99).

To determine the maximum feasible passivity indices, we analyze when (99) is positive semidefinite. Using the Schur

complement, (99) is satisfied if and only if:

$$1) \bar{\nu}_l \leq 0,$$

$$2) -\mathcal{H}(\bar{P}_l \bar{A}_l) - \bar{\rho}_l \mathbf{I}_2 - \frac{(-\bar{P}_l \bar{B}_l + \frac{1}{2} \mathbf{I}_2)^2}{-\bar{\nu}_l} \geq \mathbf{0}. \quad (100)$$

To maximize the passivity indices, we set  $\bar{\nu}_l = 0$  (the maximum value from condition 1). Then condition 2 becomes:

$$-\mathcal{H}(\bar{P}_l \bar{A}_l) - \bar{\rho}_l \mathbf{I}_2 \geq \mathbf{0}, \quad (101)$$

which requires  $-\bar{P}_l \bar{B}_l + \frac{1}{2} \mathbf{I}_2 = \mathbf{0}$ , giving  $\bar{P}_l = \frac{1}{2} \bar{B}_l^{-1}$ .

Substituting  $\bar{B}_l$  from (19) yields:

$$\bar{P}_l = \frac{L_l}{2} \mathbf{I}_2. \quad (102)$$

Now substituting (102) and  $\bar{A}_l$  from (19) into (101):

$$R_l \mathbf{I}_2 - \bar{\rho}_l \mathbf{I}_2 \geq \mathbf{0}.$$

This gives  $\bar{\rho}_l \leq R_l \mathbf{I}_2$ , and consequently the maximum feasible value is  $\bar{\rho}_l^{\max} = R_l \mathbf{I}_2$ . Therefore, the maximum feasible passivity indices are  $\bar{\nu}_l^{\max} = 0$  and  $\bar{\rho}_l^{\max} = R_l \mathbf{I}_2$  when  $\bar{P}_l = \frac{L_l}{2} \mathbf{I}_2$ . This completes the proof. ■

**Lemma 4:** For  $\tilde{\Sigma}_m^{Load}, m \in \mathbb{N}_M$  (71), the passivity indices  $\check{\nu}_m$  and  $\check{\rho}_m$  from (93) can be characterized by solving the LMI problem:

Find:  $\check{P}_m, \check{\nu}_m$ , and  $\check{\rho}_m$ ,

$$\text{s.t.: } \check{P}_m > 0, \begin{bmatrix} -\mathcal{H}(\check{P}_m \check{A}_m) - \check{\rho}_m \mathbf{I}_2 & -\check{P}_m \check{B}_m + \frac{1}{2} \mathbf{I}_2 \\ * & -\check{\nu}_m \mathbf{I}_2 \end{bmatrix} \geq \mathbf{0}, \quad (103)$$

with maximum feasible values  $\check{\nu}_m^{\max} = 0$  and  $\check{\rho}_m^{\max} = Y_{Lm} \mathbf{I}_2$  achieved when  $\check{P}_m = \frac{C_{tm}}{2} \mathbf{I}_2$ .

*Proof:* For  $\tilde{\Sigma}_m^{Load}, m \in \mathbb{N}_M$  described by (71), we establish its  $\check{X}_m$ -dissipativity with the passivity indices defined in (93). We consider the output as  $\check{y}_m = \check{x}_m$  (i.e.,  $\check{C}_m = \mathbf{I}_2$  and  $\check{D}_m = \mathbf{0}$ ). Applying Prop. 1 with the system matrices from (15) and the dissipativity supply rate form in (93), we obtain:

$$\begin{bmatrix} -\mathcal{H}(\check{P}_m \check{A}_m) + \check{C}_m^\top \check{X}_m^{22} \check{C}_m & -\check{P}_m \check{B}_m + \check{C}_m^\top \check{X}_m^{21} + \check{C}_m^\top \check{X}_m^{22} \check{D}_m \\ * & \check{X}_m^{11} + \mathcal{H}(\check{X}_m^{12} \check{D}_m) + \check{D}_m^\top \check{X}_m^{22} \check{D}_m \end{bmatrix} \geq \mathbf{0}.$$

Substituting  $\check{C}_m = \mathbf{I}_2$ ,  $\check{D}_m = \mathbf{0}$ , and the components of  $\check{X}_m$  from (93), we obtain:

$$\begin{bmatrix} -\mathcal{H}(\check{P}_m \check{A}_m) - \check{\rho}_m \mathbf{I}_2 & -\check{P}_m \check{B}_m + \frac{1}{2} \mathbf{I}_2 \\ * & -\check{\nu}_m \mathbf{I}_2 \end{bmatrix} \geq \mathbf{0},$$

which is the LMI condition (103).

To determine the maximum feasible passivity indices, we analyze when (103) is positive semidefinite. Using the Schur complement, (103) is satisfied if and only if:

$$1) \check{\nu}_m \leq 0,$$

$$2) -\mathcal{H}(\check{P}_m \check{A}_m) - \check{\rho}_m \mathbf{I}_2 - \frac{(-\check{P}_m \check{B}_m + \frac{1}{2} \mathbf{I}_2)^2}{-\check{\nu}_m} \geq \mathbf{0}. \quad (104)$$

To maximize the passivity indices, we set  $\check{\nu}_m = 0$  (the maximum value from condition 1). Then condition 2 becomes:

$$-\mathcal{H}(\check{P}_m \check{A}_m) - \check{\rho}_m \mathbf{I}_2 \geq \mathbf{0}, \quad (105)$$

which requires  $-\check{P}_m \check{B}_m + \frac{1}{2} \mathbf{I}_2 = \mathbf{0}$ , giving  $\check{P}_m = \frac{1}{2} \check{B}_m^{-1}$ . Then, by substituting  $\check{B}_m$  from (15), we get:

$$\check{P}_m = \frac{1}{2} \check{B}_m^{-1} = \frac{C_{tm}}{2} \mathbf{I}_2. \quad (106)$$

Substituting (106) and  $\check{A}_m$  from (15) into (105) and

computing,  $\mathcal{H}(\check{P}_m \check{A}_m)$ , we get:

$$\mathcal{H}(\check{P}_m \check{A}_m) = -Y_{Lm} \mathbf{I}_2,$$

which yields:

$$-\mathcal{H}(\check{P}_m \check{A}_m) - \check{\rho}_m \mathbf{I}_2 = Y_{Lm} \mathbf{I}_2 - \check{\rho}_m \mathbf{I}_2 \geq 0.$$

This gives  $\check{\rho}_m \leq Y_{Lm} \mathbf{I}_2$ . Therefore, the maximum feasible passivity indices are  $\check{\nu}_m^{\max} = 0$  and  $\check{\rho}_m^{\max} = Y_{Lm} \mathbf{I}_2$  when  $\check{P}_m = \frac{C_{tm}}{2} \mathbf{I}_2$ . This completes the proof.  $\blacksquare$

#### A. Global Control and Topology Co-design

The local controllers (21) regulate voltages of individual DGs while ensuring that closed-loop DG dynamics satisfy the required dissipativity properties established in Th. 2. Given these subsystem properties, we now synthesize the distributed controller gains and communication topology by designing the interconnection matrix block  $\tilde{K}$  in (77) using Proposition 2.

Note that by designing  $\tilde{K} = [\tilde{K}_{ij}]_{i,j \in \mathbb{N}_N}$  in the error interconnection matrix  $\tilde{M}$  (77), we can uniquely determine the consensus-based distributed global controller gains  $\{K_{ij}^P, K_{ij}^Q, K_{ij}^\Omega : i, j \in \mathbb{N}_N\}$  from (37)-(39), along with the required communication topology  $\mathcal{G}^c$ . Specifically, when designing  $\tilde{K}$ , we enforce two structural constraints: (i) each off-diagonal block  $\tilde{K}_{ij}$  (for  $j \neq i$ ) maintains the structure of the corresponding  $\tilde{K}_{ij}$  block with three inner zero blocks as shown in (37), and (ii) each diagonal block  $\tilde{K}_{ii}$  satisfies the balance condition (39).

We design the closed-loop networked error dynamics of the AC MG (shown in Fig. 6) to be finite-gain  $L_2$ -stable with an  $L_2$ -gain  $\gamma$  from disturbance  $w_c(t)$  to performance output  $z_c(t)$ , where  $\gamma$  is prespecified such that  $\tilde{\gamma} \triangleq \gamma^2 < \bar{\gamma}$ . This corresponds to making the system  $\mathbf{Y}$ -dissipative with  $\mathbf{Y} \triangleq \begin{bmatrix} \gamma^2 \mathbf{I} & 0 \\ 0 & -\mathbf{I} \end{bmatrix}$  (see Remark 1), which prevents/bounds the amplification of disturbances affecting system performance. The following theorem formulates this distributed global controller and communication topology co-design problem.

**Theorem 3:** The closed-loop networked error dynamics of the AC MG (see Fig. 6) can be made finite-gain  $L_2$ -stable with an  $L_2$ -gain  $\gamma$  from disturbance  $w_c(t)$  to performance output  $z_c(t)$  (where  $\tilde{\gamma} \triangleq \gamma^2 < \bar{\gamma}$  is prespecified), by synthesizing the interconnection matrix block  $\tilde{K}$  in (77) via solving the LMI problem:

$$\min_{Q, \{p_i : i \in \mathbb{N}_N\}, \{\bar{\rho}_l : l \in \mathbb{N}_L\}, \{\check{\rho}_m : m \in \mathbb{N}_M\}, \tilde{\gamma}} \sum_{i,j \in \mathbb{N}_N} c_{ij} \|Q_{ij}\|_1 + c_0 \tilde{\gamma},$$

$$\text{Sub. to: } p_i > 0, \bar{\rho}_l > 0, \check{\rho}_m > 0,$$

$$0 < \tilde{\gamma} < \bar{\gamma}, \text{ and the LMI (108) } > 0, \quad (107)$$

where  $K = (\mathbf{X}_p^{11})^{-1} Q$ ,  $\mathbf{X}^{12} \triangleq \text{diag}([- \frac{1}{2\nu_i} \mathbf{I}]_{i \in \mathbb{N}_N})$ ,  $\mathbf{X}^{21} \triangleq (\mathbf{X}^{12})^\top$ ,  $\bar{\mathbf{X}}^{12} \triangleq \text{diag}([- \frac{1}{2\bar{\nu}_l} \mathbf{I}]_{l \in \mathbb{N}_L})$ ,  $\bar{\mathbf{X}}^{21} \triangleq (\bar{\mathbf{X}}^{12})^\top$ ,  $\check{\mathbf{X}}^{12} \triangleq \text{diag}([- \frac{1}{2\check{\nu}_m} \mathbf{I}]_{m \in \mathbb{N}_M})$ ,  $\check{\mathbf{X}}^{21} \triangleq (\check{\mathbf{X}}^{12})^\top$ ,  $\mathbf{X}_p^{11} \triangleq \text{diag}([-p_i \nu_i \mathbf{I}]_{i \in \mathbb{N}_N})$ ,  $\mathbf{X}_p^{22} \triangleq \text{diag}([-p_i \rho_i \mathbf{I}]_{i \in \mathbb{N}_N})$ ,  $\bar{\mathbf{X}}_{\bar{p}}^{11} \triangleq \text{diag}([- \bar{\rho}_l \bar{\nu}_l \mathbf{I}]_{l \in \mathbb{N}_L})$ ,  $\bar{\mathbf{X}}_{\bar{p}}^{22} \triangleq \text{diag}([- \bar{\rho}_l \bar{\rho}_l \mathbf{I}]_{l \in \mathbb{N}_L})$ ,  $\check{\mathbf{X}}_{\check{p}}^{11} \triangleq \text{diag}([- \check{\rho}_m \check{\nu}_m \mathbf{I}]_{m \in \mathbb{N}_M})$ ,  $\check{\mathbf{X}}_{\check{p}}^{22} \triangleq \text{diag}([- \check{\rho}_m \check{\rho}_m \mathbf{I}]_{m \in \mathbb{N}_M})$ , and  $\tilde{\Gamma} \triangleq \tilde{\gamma} \mathbf{I}$ . The structure of  $Q \triangleq [Q_{ij}]_{i,j \in \mathbb{N}_N}$  mirrors  $K \triangleq$

$[K_{ij}]_{i,j \in \mathbb{N}_N}$  (with zeros in appropriate blocks). The coefficients  $c_0 > 0$  and  $c_{ij} > 0, \forall i, j \in \mathbb{N}_N$  weight disturbance attenuation and communication costs.

*Proof:* The proof follows directly from applying Proposition 2 to the networked error system with interconnection matrix  $\tilde{M}$  defined in (77). The DG subsystems are characterized as  $X_i$ -EID with passivity indices from Theorem 2, the line subsystems as  $\bar{X}_l$ -EID with passivity indices from Lemma 3, and the load subsystems as  $\check{X}_m$ -EID with passivity indices from Lemma 4. The desired  $L_2$ -stability property corresponds to  $\mathbf{Y}$ -dissipativity with  $\mathbf{Y} \triangleq \begin{bmatrix} \gamma^2 \mathbf{I} & 0 \\ 0 & -\mathbf{I} \end{bmatrix}$ , which satisfies Assumption 1 since  $\mathbf{Y}^{22} = -\mathbf{I} < 0$ . All subsystems satisfy Assumption 2 since their  $X^{11}$  blocks are positive definite (as  $\nu_i < 0$ ,  $\bar{\nu}_l < 0$ ,  $\check{\nu}_m < 0$  from the passivity conditions). Applying Proposition 2 with these dissipativity properties yields the LMI (108), where the decision variables are the multipliers  $\{p_i, \bar{\rho}_l, \check{\rho}_m\}$  and the interconnection structure encoded in  $Q$ . The objective function trades off communication sparsity (via  $\ell_1$ -norm) and disturbance rejection performance (via  $\tilde{\gamma}$ ). Upon solving (107), the distributed controller gains are recovered through the relationships (37)-(39). This completes the proof.  $\blacksquare$

#### B. Local Controller Synthesis

To ensure the necessary LMI conditions from Theorem 2, Lemma 3, and Lemma 4 on subsystem passivity indices hold and to guarantee numerical feasibility of the global co-design problem (107), we must first synthesize the local controllers for DG subsystems and verify that line and load subsystems achieve their required passivity properties. This local synthesis determines the achievable passivity indices  $\{\nu_i, \rho_i : i \in \mathbb{N}_N\}$ ,  $\{\bar{\nu}_l, \bar{\rho}_l : l \in \mathbb{N}_L\}$ , and  $\{\check{\nu}_m, \check{\rho}_m : m \in \mathbb{N}_M\}$  that will be used in the global co-design.

For the line and load subsystems, Lemma 3 and Lemma 4 provide analytical expressions for the maximum achievable passivity indices based on physical parameters. Specifically, we have  $\bar{\nu}_l^{\max} = 0$  and  $\bar{\rho}_l^{\max} = R_l \mathbf{I}_2$  for line subsystem  $l \in \mathbb{N}_L$ , and  $\check{\nu}_m^{\max} = 0$  and  $\check{\rho}_m^{\max} = Y_{Lm} \mathbf{I}_2$  for load subsystem  $m \in \mathbb{N}_M$ . These maximum values are achieved with  $\bar{P}_l = \frac{L_l}{2} \mathbf{I}_2$  and  $\check{P}_m = \frac{C_{tm}}{2} \mathbf{I}_2$ , respectively, and can be directly used in the global co-design without additional optimization.

For DG subsystems, however, the achievable passivity indices depend on the local controller gains,  $\{K_{i0} : i \in \mathbb{N}_N\}$  which must be synthesized to satisfy Theorem 2 while ensuring compatibility with the global design parameters from (107). The following theorem formalizes this local controller synthesis problem.

**Theorem 4:** Given the DG parameters (36), line parameters (19), load parameters (15), and frequency coupling bounds  $\{\beta_i : i \in \mathbb{N}_N\}$  from Lemma 2, the local controller gains  $\{K_{i0}, i \in \mathbb{N}_N\}$  from (21) can be synthesized along with the DG passivity indices  $\{\nu_i, \rho_i : i \in \mathbb{N}_N\}$ , line passivity indices  $\{\bar{\nu}_l, \bar{\rho}_l : l \in \mathbb{N}_L\}$ , and load passivity indices  $\{\check{\nu}_m, \check{\rho}_m : m \in \mathbb{N}_M\}$  to ensure feasibility of the global co-

design problem (107) by solving:

Find:  $\{(\tilde{K}_{i0}, \tilde{P}_i, \tilde{R}_i, \tilde{\lambda}_i, \nu_i, \tilde{\rho}_i) : i \in \mathbb{N}_N\}$ ,  
 $\{(\bar{P}_l, \bar{\nu}_l, \bar{\rho}_l) : l \in \mathbb{N}_L\}$ , and  $\{(\check{P}_m, \check{\nu}_m, \check{\rho}_m) : m \in \mathbb{N}_M\}$   
s.t.:  $\tilde{P}_i > 0, \tilde{R}_i > 0, \tilde{\lambda}_i > 0, \nu_i < 0, \tilde{\rho}_i > 0, \forall i \in \mathbb{N}_N$ ,  
 $\bar{P}_l > 0, \forall l \in \mathbb{N}_L, \quad \check{P}_m > 0, \forall m \in \mathbb{N}_M$ ,

$$\begin{bmatrix} \Phi_i & \tilde{R}_i & \mathbf{0} & \mathbf{0} \\ \tilde{R}_i & \tilde{R}_i & \tilde{P}_i & \mathbf{0} \\ \mathbf{0} & \tilde{P}_i & -\mathcal{H}(A_i \tilde{P}_i + B_i \tilde{K}_{i0}) + \tilde{\lambda}_i \mathbf{I} & -\mathbf{I} + \frac{1}{2} \tilde{P}_i \\ \mathbf{0} & \mathbf{0} & -\mathbf{I} + \frac{1}{2} \tilde{P}_i & -\nu_i \mathbf{I} \end{bmatrix} > \mathbf{0},$$

$$\begin{bmatrix} -\mathcal{H}(\bar{P}_l \bar{A}_l) - \bar{\rho}_l \mathbf{I}_2 & -\bar{P}_l \bar{B}_l + \frac{1}{2} \mathbf{I}_2 \\ * & -\bar{\nu}_l \mathbf{I}_2 \end{bmatrix} \geq \mathbf{0}, \quad \forall l \in \mathbb{N}_L,$$

$$\begin{bmatrix} -\mathcal{H}(\check{P}_m \check{A}_m) - \check{\rho}_m \mathbf{I}_2 & -\check{P}_m \check{B}_m + \frac{1}{2} \mathbf{I}_2 \\ * & -\check{\nu}_m \mathbf{I}_2 \end{bmatrix} \geq \mathbf{0}, \quad \forall m \in \mathbb{N}_M,$$

where  $\Phi_i \triangleq \tilde{\rho}_i \mathbf{I} + \tilde{R}_i - \tilde{\lambda}_i \beta_i^2 e_7 e_7^T$ ,  $K_{i0} \triangleq \tilde{K}_{i0} P_i^{-1}$ , and  $\rho_i \triangleq \frac{1}{\tilde{\rho}_i}$ .

*Proof:* The local synthesis ensures three requirements: (1) each DG error subsystem  $\tilde{\Sigma}_i^{DG}$  satisfies IF-OFP( $\nu_i, \rho_i$ ) via Theorem 2, (2) each line error subsystem  $\tilde{\Sigma}_l^{line}$  satisfies IF-OFP( $\bar{\nu}_l, \bar{\rho}_l$ ) via Lemma 3, and (3) each load error subsystem  $\tilde{\Sigma}_m^{Load}$  satisfies IF-OFP( $\check{\nu}_m, \check{\rho}_m$ ) via Lemma 4. The LMI constraints directly follow from these theorems and lemmas. For DG subsystems, the constraints ensure local stability through storage function  $V_i(\tilde{x}_i) = \tilde{x}_i^T P_i \tilde{x}_i$  (where  $P_i = \tilde{P}_i^{-1}$ ) while satisfying the frequency coupling constraint via the S-procedure with multiplier  $\lambda_i = \tilde{\lambda}_i^{-1}$ . For line and load subsystems, the constraints verify achievable passivity regions. Compatibility with the global co-design (107) is ensured through passivity index requirements:  $\nu_i < 0$  and  $\rho_i > 0$  ensure  $X_p^{11} = \text{diag}([-p_i \nu_i \mathbf{I}]_{i \in \mathbb{N}_N}) > 0$  and  $X_p^{22} = \text{diag}([-p_i \rho_i \mathbf{I}]_{i \in \mathbb{N}_N}) > 0$  for any  $p_i > 0$ , and similarly for line and load passivity indices. Upon solving this unified LMI problem, the actual local controller gains are recovered as  $K_{i0} = \tilde{K}_{i0} \tilde{P}_i^{-1}$  and output passivity indices as  $\rho_i = \tilde{\rho}_i^{-1}$ , which are then used in the global co-design (107). ■

## VII. CONCLUSION

This paper presents a dissipativity-based framework for co-designing distributed controllers and communication topologies in AC microgrids. The approach formulates the closed-loop AC MG as a networked system and employs a hierarchical control architecture that combines local PI controllers with distributed consensus-based controllers for droop-free proportional power sharing. We establish necessary and sufficient conditions for subsystem passivity that account for coupled dq-frame dynamics and frequency coupling nonlinearity. The co-design problem is formulated as a convex optimization that simultaneously synthesizes

distributed controller gains and sparse communication topology while guaranteeing system stability. Equilibrium point analysis provides conditions for achieving voltage regulation, frequency synchronization, and proportional power sharing at steady state.

## REFERENCES

- [1] Y. Han, H. Li, P. Shen, E. A. A. Coelho, and J. M. Guerrero, "Review of active and reactive power sharing strategies in hierarchical controlled microgrids," *IEEE Transactions on Power Electronics*, vol. 32, no. 3, pp. 2427–2451, 2016.
- [2] D. E. Olivares, A. Mehrizi-Sani, A. H. Etemadi, C. A. Cañizares, R. Iravani, M. Kazerani, A. H. Hajimiragha, O. Gomis-Bellmunt, M. Saeedifard, R. Palma-Behnke *et al.*, "Trends in microgrid control," *IEEE Transactions on smart grid*, vol. 5, no. 4, pp. 1905–1919, 2014.
- [3] J. Rocabert, A. Luna, F. Blaabjerg, and P. Rodriguez, "Control of power converters in ac microgrids," *IEEE transactions on power electronics*, vol. 27, no. 11, pp. 4734–4749, 2012.
- [4] S. Sahoo, T. Dragičević, and F. Blaabjerg, "Cyber security in control of grid-tied power electronic converters—challenges and vulnerabilities," *IEEE Journal of Emerging and Selected Topics in Power Electronics*, vol. 9, no. 5, pp. 5326–5340, 2019.
- [5] A. Bidram and A. Davoudi, "Hierarchical structure of microgrids control system," *IEEE Transactions on Smart Grid*, vol. 3, no. 4, pp. 1963–1976, 2012.
- [6] Q. Shafiee, J. M. Guerrero, and J. C. Vasquez, "Distributed secondary control for islanded microgrids—a novel approach," *IEEE Transactions on power electronics*, vol. 29, no. 2, pp. 1018–1031, 2013.
- [7] F. Guo, C. Wen, J. Mao, and Y.-D. Song, "Distributed secondary voltage and frequency restoration control of droop-controlled inverter-based microgrids," *IEEE Transactions on industrial Electronics*, vol. 62, no. 7, pp. 4355–4364, 2014.
- [8] S. Zuo, A. Davoudi, Y. Song, and F. L. Lewis, "Distributed finite-time voltage and frequency restoration in islanded ac microgrids," *IEEE Transactions on Industrial Electronics*, vol. 63, no. 10, pp. 5988–5997, 2016.
- [9] J. W. Simpson-Porco, F. Dörfler, and F. Bullo, "Voltage stabilization in microgrids via quadratic droop control," *IEEE Transactions on Automatic Control*, vol. 62, no. 3, pp. 1239–1253, 2016.
- [10] M. Arcak, C. Meissen, and A. Packard, *Networks of dissipative systems: compositional certification of stability, performance, and safety*. Springer, 2016.
- [11] C. De Persis and N. Monshizadeh, "Bregman storage functions for microgrid control," *IEEE Transactions on Automatic Control*, vol. 63, no. 1, pp. 53–68, 2017.
- [12] A. Kwasinski and P. T. Krein, "Stabilization of constant power loads in dc–dc converters using passivity-based control," in *INTELEC 07-29th International Telecommunications Energy Conference*. IEEE, 2007, pp. 867–874.
- [13] J. Schiffer, D. Zonetti, R. Ortega, A. M. Stanković, T. Sezi, and J. Raisch, "A survey on modeling of microgrids—from fundamental physics to phasors and voltage sources," *Automatica*, vol. 74, pp. 135–150, 2016.
- [14] S. Trip and C. De Persis, "Distributed optimal load frequency control with non-passive dynamics," *IEEE Transactions on Control of Network Systems*, vol. 5, no. 3, pp. 1232–1244, 2017.
- [15] L. Meng, Q. Shafiee, G. F. Trecate, H. Karimi, D. Fulwani, X. Lu, and J. M. Guerrero, "Review on control of dc microgrids and multiple microgrid clusters," *IEEE journal of emerging and selected topics in power electronics*, vol. 5, no. 3, pp. 928–948, 2017.

$$\begin{bmatrix} \mathbf{X}_p^{11} & \mathbf{0} & \mathbf{0} & Q & \mathbf{X}_p^{11} \bar{C} \\ \mathbf{0} & \bar{\mathbf{X}}_{\bar{p}}^{11} & \mathbf{0} & \bar{\mathbf{X}}_{\bar{p}}^{11} C & \mathbf{0} \\ \mathbf{0} & \mathbf{0} & \bar{\mathbf{X}}_{\bar{p}}^{11} & \mathbf{0} & \mathbf{0} \\ Q^T & C^T \bar{\mathbf{X}}_{\bar{p}}^{11} & \mathbf{0} & -Q^T \mathbf{X}^{12} - \mathbf{X}^{21} Q - \mathbf{X}_p^{22} & -\mathbf{X}^{21} \mathbf{X}_p^{11} \bar{C} - C^T \bar{\mathbf{X}}_{\bar{p}}^{11} \bar{\mathbf{X}}^{12} \\ \bar{C}^T \mathbf{X}_p^{11} & \mathbf{0} & \mathbf{0} & -\bar{C}^T \mathbf{X}_p^{11} \mathbf{X}^{12} - \bar{\mathbf{X}}^{21} \bar{\mathbf{X}}_{\bar{p}}^{11} C & -\bar{\mathbf{X}}_{\bar{p}}^{22} \\ \mathbf{0} & \bar{C}^T \bar{\mathbf{X}}_{\bar{p}}^{11} & \bar{C}^T \bar{\mathbf{X}}_{\bar{p}}^{11} & \mathbf{0} & -\bar{C}^T \bar{\mathbf{X}}_{\bar{p}}^{11} \mathbf{X}^{12} - \bar{\mathbf{X}}^{21} \bar{\mathbf{X}}_{\bar{p}}^{11} \bar{C} \\ B_c^T \mathbf{X}_p^{11} & \bar{E}_c^T \bar{\mathbf{X}}_{\bar{p}}^{11} & \bar{E}_c^T \bar{\mathbf{X}}_{\bar{p}}^{11} & -E_c^T \mathbf{X}_p^{11} \mathbf{X}^{12} - H_c & -E_c^T \mathbf{X}_p^{11} \bar{C} - \bar{E}_c^T \bar{\mathbf{X}}_{\bar{p}}^{11} \mathbf{X}^{12} - \bar{H}_c \end{bmatrix} \begin{bmatrix} \mathbf{0} \\ \bar{\mathbf{X}}_{\bar{p}}^{11} \bar{C} \\ \bar{\mathbf{X}}_{\bar{p}}^{11} \bar{C} \\ \mathbf{0} \\ -\mathbf{X}^{21} \bar{\mathbf{X}}_{\bar{p}}^{11} \bar{C} \\ -\bar{\mathbf{X}}^{21} \bar{\mathbf{X}}_{\bar{p}}^{11} \bar{C} \\ \mathbf{0} \\ -\bar{C}^T \mathbf{X}_p^{11} E_c - \bar{\mathbf{X}}^{21} \bar{\mathbf{X}}_{\bar{p}}^{11} \bar{E}_c - \bar{H}_c^T \\ -\bar{C}^T \bar{\mathbf{X}}_{\bar{p}}^{11} E_c - \bar{\mathbf{X}}^{21} \bar{\mathbf{X}}_{\bar{p}}^{11} \bar{E}_c - \bar{H}_c^T \\ \bar{C}^T \bar{\mathbf{X}}_{\bar{p}}^{11} \bar{C} \\ \bar{E}^T \bar{\mathbf{X}}_{\bar{p}}^{11} \bar{C} \end{bmatrix} \begin{bmatrix} \mathbf{X}_p^{11} E_c \\ \bar{\mathbf{X}}_{\bar{p}}^{11} \bar{E}_c \\ \bar{\mathbf{X}}_{\bar{p}}^{11} \bar{E}_c \\ -\mathbf{X}^{21} \bar{\mathbf{X}}_{\bar{p}}^{11} E_c - H_c^T \\ -\bar{C}^T \mathbf{X}_p^{11} E_c - \bar{\mathbf{X}}^{21} \bar{\mathbf{X}}_{\bar{p}}^{11} \bar{E}_c - \bar{H}_c^T \\ -\bar{C}^T \bar{\mathbf{X}}_{\bar{p}}^{11} E_c - \bar{\mathbf{X}}^{21} \bar{\mathbf{X}}_{\bar{p}}^{11} \bar{E}_c - \bar{H}_c^T \\ \bar{C}^T \bar{\mathbf{X}}_{\bar{p}}^{11} \bar{C} \\ \bar{E}^T \bar{\mathbf{X}}_{\bar{p}}^{11} \bar{C} \end{bmatrix} \quad (108)$$

- [16] Y. Khayat, Q. Shafiee, R. Heydari, M. Naderi, T. Dragičević, J. W. Simpson-Porco, F. Dörfler, M. Fathi, F. Blaabjerg, J. M. Guerrero *et al.*, “On the secondary control architectures of ac microgrids: An overview,” *IEEE Transactions on Power Electronics*, vol. 35, no. 6, pp. 6482–6500, 2019.
- [17] M. J. Najafirad and S. Welikala, “Dissipativity-based distributed droop-free control and communication topology co-design for dc microgrids,” in *2025 American Control Conference (ACC)*. IEEE, 2025, pp. 1153–1160.
- [18] S. Welikala, Z. Song, H. Lin, and P. J. Antsaklis, “Decentralized co-design of distributed controllers and communication topologies for vehicular platoons: A dissipativity-based approach,” *Automatica*, vol. 174, p. 112118, 2025.
- [19] M. Arcak, “Compositional Design and Verification of Large-Scale Systems Using Dissipativity Theory: Determining Stability and Performance From Subsystem Properties and Interconnection Structures,” *IEEE Control Systems Magazine*, vol. 42, no. 2, pp. 51–62, 2022.
- [20] S. Welikala, H. Lin, and P. J. Antsaklis, “Non-linear networked systems analysis and synthesis using dissipativity theory,” in *2023 American Control Conference (ACC)*. IEEE, 2023, pp. 2951–2956.
- [21] ———, “On-line estimation of stability and passivity metrics,” in *2022 IEEE 61st Conference on Decision and Control (CDC)*. IEEE, 2022, pp. 267–272.
- [22] P. Nahata and G. Ferrari-Treeate, “Passivity-based voltage and frequency stabilization in ac microgrids,” in *2019 18th European Control Conference (ECC)*. IEEE, 2019, pp. 1890–1895.
- [23] H. S. Khan and A. Y. Memon, “Active and reactive power control of the voltage source inverter in an ac microgrid,” *Sustainability*, vol. 15, no. 2, p. 1621, 2023.
- [24] K. Zuo and L. Wu, “An asymptotic stability guaranteed droop-free control scheme for normalized power consensus in microgrids,” in *2023 IEEE Power & Energy Society General Meeting (PESGM)*. IEEE, 2023, pp. 1–5.